

mTORC2 Is Required for Proliferation and Survival of TSC2-Null Cells[∇]

Elena A. Goncharova,¹ Dmitry A. Goncharov,¹ Hua Li,¹ Wittaya Pimpong,¹
Stephen Lu,¹ Irene Khavin,¹ and Vera P. Krymskaya^{1,2,3*}

Pulmonary, Allergy and Critical Care Division, Department of Medicine,¹ Abramson Cancer Center,² and Cardiovascular Institute,³ University of Pennsylvania, Philadelphia, Pennsylvania

Received 10 September 2010/Returned for modification 19 November 2010/Accepted 29 March 2011

Mutational inactivation of the tumor suppressor tuberous sclerosis complex 2 (TSC2) constitutively activates mTORC1, increases cell proliferation, and induces the pathological manifestations observed in tuberous sclerosis (TS) and in pulmonary lymphangioleiomyomatosis (LAM). While the role of mTORC1 in TSC2-dependent growth has been extensively characterized, little is known about the role of mTORC2. Our data demonstrate that mTORC2 modulates TSC2-null cell proliferation and survival through RhoA GTPase and Bcl2 proteins. TSC2-null cell proliferation was inhibited not only by reexpression of TSC2 or small interfering RNA (siRNA)-induced downregulation of Rheb, mTOR, or raptor, but also by siRNA for rictor. Increased RhoA GTPase activity and P-Ser473 Akt were inhibited by siRNA for rictor. Importantly, constitutively active V14RhoA reversed growth inhibition induced by siRNA for rictor, siRNA TSC1, reexpression of TSC2, or simvastatin. While siRNA for RhoA had a modest effect on growth inhibition, downregulation of RhoA markedly increased TSC2-null cell apoptosis. Inhibition of RhoA activity downregulated antiapoptotic Bcl2 and upregulated proapoptotic Bim, Bok, and Puma. *In vitro* and *in vivo*, simvastatin alone or in combination with rapamycin inhibited cell growth and induced TSC2-null cell apoptosis, abrogated TSC2-null tumor growth, improved animal survival, and prevented tumor recurrence by inhibiting cell growth and promoting apoptosis. Our data demonstrate that mTORC2-dependent activation of RhoA is required for TSC2-null cell growth and survival and suggest that targeting both mTORC2 and mTORC1 by a combination of proapoptotic simvastatin and cytostatic rapamycin shows promise for combinational therapeutic intervention in diseases with TSC2 dysfunction.

Mutational inactivation of the tumor suppressor gene *tuberous sclerosis complex 2 (TSC2)* occurs in hamartoma syndrome tuberous sclerosis (TS) and pulmonary lymphangioleiomyomatosis (LAM). TS manifests as multiple tumors in the brain, kidney, heart, and skin (33). LAM, a rare lung disease predominantly affecting women, which can be sporadic or associated with TS, manifests by neoplastic growth of atypical smooth muscle LAM cells, lung cyst formation, obstruction of lymphatics, and spontaneous pneumothoraces (33, 46, 85). A major advance in understanding TS and LAM occurred with the discovery of TSC2 as a negative regulator of the mammalian target of rapamycin complex 1 (mTORC1) (30, 32, 50, 54, 59, 93). TSC2 forms a tumor suppressor complex with TSC1 and regulates mTORC1 by directly controlling the activity of the small GTPase Rheb via the GTPase-activating protein (GAP) domain of TSC2 (9, 24, 43, 95). Rheb binds to raptor and controls the activity of mTORC1, which directly phosphorylates p70 S6 kinase (S6K1) and 4E-BP1 (57, 63). Importantly, the constitutive activation of S6K1 promotes a negative-feedback loop that also inhibits phosphatidylinositol 3-kinase (PI3K) activity (37, 80, 88). Activation of mTORC1 is sensitive to inhibition by rapamycin, which has been used in the

treatment of TS and LAM (35). Rapamycin treatment induced regression of astrocytomas in TS (21) and markedly improved pulmonary functions and reduced the size of angiomyolipomas (AML) in LAM-TS patients (3). Unfortunately, cessation of rapamycin therapy resulted in the regrowth of subependymal giant cell astrocytomas (21) and the return of diminished pulmonary function and AML tumors to the state observed prior to rapamycin treatment (3). Accordingly, alternative or combinational therapies are needed to treat diseases with mutational inactivation of TSC2.

The mTOR forms two functionally distinct multiprotein complexes, mTORC1 and mTORC2, that control cell growth, proliferation, and survival. Both mTORC1 and mTORC2 are critical for embryonic development (36, 81). Further, the rapamycin-sensitive mTORC1 has an evolutionarily conserved function in regulating cell growth, cell cycle progression, and cell proliferation (20). While both mTORC1 and mTORC2 are required for cell growth in yeast (64), little is known about the role of mTORC2 in increased cell proliferation due to TSC2 loss. The first established function of TORC2 was the rapamycin-insensitive cell cycle-dependent regulation of actin cytoskeleton through activation of Rho GTPase (76, 77). Identification of mTORC2 in mammals confirmed its rapamycin-insensitive regulation of actin cytoskeleton through the Rho GTPases RhoA and Rac1 (44, 75). The Rho family of small GTPases consists of three major members, RhoA, Rac1, and Cdc42 (16). In its GTP-bound state, activated RhoA promotes stress fiber and focal-adhesion formation. TSC1 forms a tumor suppressor complex with TSC2 and promotes stress fiber formation through activation of RhoA GTPase

* Corresponding author. Mailing address: Pulmonary, Allergy and Critical Care Division, Department of Medicine, University of Pennsylvania, Translational Research Laboratories, 125 South 31st Street, Room 1212, Philadelphia, PA 19104. Phone: (215) 573-9861. Fax: (215) 746-1224. E-mail: krymskay@mail.med.upenn.edu.

[∇] Published ahead of print on 11 April 2011.

(56). We demonstrated that loss of TSC2 induces a rapamycin-insensitive increase in stress fiber formation due to activation of RhoA GTPase that is inhibited by reexpression of TSC2 or small interfering RNA (siRNA) for TSC1 (27, 31). Whether TSC2 regulates the actin cytoskeleton through mTORC2 activation and/or whether TSC2-dependent activation of Rho is required for increased TSC2-null cell proliferation remains unknown.

The biochemical functions of Rho GTPases in regulating the actin cytoskeleton and cell adhesion translate into biological functions, including regulation of cell proliferation, migration, and morphogenesis (45). Geranylgeranylation of Rho GTPase ensures membrane localization and activation (74) that can be affected by statins, small-molecule inhibitors of 3-hydroxy-3-methylglutaryl coenzyme A (HMG-CoA) reductase. Statins modulate lipid metabolism and geranylgeranylation of Rho GTPase (58, 73) and induce apoptosis and inhibit proliferation in various cancer cell lines and human smooth muscle cells (22, 23, 48, 66, 71, 84, 91). Importantly, statins synergize with rapamycin and its analogs in inhibiting proliferation and inducing apoptosis in leukemia, prostate and breast cancer, and rat smooth muscle cells (6, 8, 17, 70). Interestingly, atorvastatin had little effect on syngeneic TSC2^{-/-} mouse embryonic fibroblast (MEF) subcutaneous tumors in nude mice (61). In this study, we utilized TSC2-null ELT3 cells derived from spontaneous uterine leiomyoma (38) of the Eker rat, a naturally occurring animal model with germ line TSC2 gene mutation (51). In our published studies, we have also demonstrated that in ELT3 cells, loss of TSC2 increased proliferation due to constitutively active mTORC1 (30) and activated Rho GTPase due to TSC1-dependent inhibition of Rac1 (27). Whether TSC2-dependent Rho activation acts through mTORC2 and is required for increased TSC2-null cell proliferation has not been investigated.

In this study, we present evidence that mTORC2-dependent RhoA GTPase activation is necessary for increased TSC2-null cell proliferation and survival. We found that siRNA for rictor inhibits both increased RhoA activity and increased P-Ser473 Akt in TSC2-null ELT3 cells and smooth-muscle-like cells derived from LAM lungs. Additionally, siRNA for rictor and siRNA for RhoA inhibit TSC2-null cell proliferation, and expression of constitutively active RhoA rescued TSC2- and rictor siRNA-dependent inhibition of DNA synthesis. We also show that combined targeting of RhoA GTPase with simvastatin and mTORC1 with rapamycin inhibits TSC2-null cell proliferation, induces apoptosis, abrogates TSC2-null tumor growth, and prevents tumor recurrence after simvastatin or the combination of simvastatin with rapamycin treatment was withdrawn. Our data suggest that combined inhibition of RhoA by simvastatin and mTORC1 by rapamycin may be beneficial for inhibiting TSC2-related tumorigenesis and for preventing posttreatment tumor recurrence in LAM and TS.

MATERIALS AND METHODS

Cell culture. TSC2-null ELT3 cell, derived from the Eker rat uterine leiomyoma (38) were generously provided to us by Cheryl Walker, M. D. Anderson Cancer Center, University of Texas, Smithville, TX, and maintained as previously described (18, 28, 30). A littermate-derived pair of Tsc2^{+/+} p53^{-/-} and Tsc2^{-/-} p53^{-/-} MEFs with p53 deleted for immortalization and isogenic Tsc2^{-/-} and Tsc2^{+/+} MEFs with reconstituted TSC2 were generously provided by D. J. Kwiatkowski (Brigham and Women's Hospital, Boston, MA) and were maintained in Dulbecco's modified Eagle's medium (DMEM) with 10% fetal bovine serum (FBS) (94). LAM-derived (LAMd) cells were dissociated from LAM

nodules from the lungs of LAM patients who had undergone lung transplantation, as described previously (30), and obtained from the National Disease Research Interchange (Philadelphia, PA) according to approved protocol. LAMd cells in subculture during the 3rd through 12th passages were used. All experiments were performed with a minimum of three different LAMd cell cultures. Prior to the start of experiments, cells were serum deprived for 24 h.

Microinjection. Microinjection was performed using the Eppendorf Microinjection System (Hamburg, Germany) as described previously (27, 30). Briefly, specific siRNA from Dharmacon, Inc. (Lafayette, CO), directed against Rheb, mTOR, raptor, or rictor or scrambled siRNA was comicroinjected with green fluorescent protein (GFP) or glutathione S-transferase (GST) to identify microinjected cells; 30 to 42 h postinjection, the cells were serum deprived overnight, followed by immunocytochemical or bromodeoxyuridine (BrdU) incorporation analysis.

Immunocytochemistry. Cells were washed 3 times with phosphate-buffered saline (PBS), fixed with 3.7% paraformaldehyde for 15 min, treated with 0.1% Triton X-100 for 30 min at room temperature, and blocked with 2% bovine serum albumin (BSA) in PBS for 60 min. After incubation with rhodamine-phalloidin (Molecular Probes, Eugene, OR) or primary and then secondary antibodies conjugated with either Alexa Fluor 488, Alexa Fluor 594, or Alexa Fluor 633, the cells were mounted in Vectashield mounting medium (Vector Laboratories, Burlingame, CA). Immunostaining was analyzed using a Nikon Eclipse TE2000-E microscope equipped with an Evolution QEi digital video camera or using a Nikon Eclipse E400 microscope equipped with a Nikon Coolpix 995 digital camera under $\times 200$ magnification.

Transient transfection, preparation of cell lysates, and immunoblot analysis. pEGFP, pEGFP-TSC2, pEBG, and pEBG-V14RhoA expression vectors were prepared using the EndoFree Plasmid Maxi kit (Qiagen, Valencia, CA). siRNA GLO, scrambled siRNA, and siRNA for Rho, mTOR, rictor, or raptor were purchased from Dharmacon RNA Technologies (Lafayette, CO). Transient transfection was performed using Effectene or RNAiFect transfection reagent (Qiagen) according to the manufacturer's protocols as described previously (27, 29). For siRNA transfection, serum-deprived cells were incubated for 48 or 72 h with specific or control siRNA, followed by the DNA synthesis assay or the analysis of apoptosis. Reexpression of GFP-TSC2 and depletion of RhoA, rictor, or raptor were verified by immunoblot analysis with anti-tuberin (Santa Cruz Biotechnology, Inc., Santa Cruz, CA), anti-RhoA, anti-raptor (Cell Signaling Technology), anti-rictor (Affinity Bioreagents), or anti-total actin (Sigma-Aldrich, Inc., St. Louis, MO) antibodies. For immunoblot analysis, siRNA for Rheb, mTOR, raptor, or rictor was introduced using RNAiFect transfection reagents (Qiagen). As a control, we used scrambled and siGLO RISC-Free siRNA (Dharmacon, Inc., Lafayette, CO). Apoptotic immunoblot analyses were performed using phospho-Ser46 p53, total p53, cleaved caspase 3 antibodies, and a proapoptotic Bcl-2 family antibody kit purchased from Cell Signaling Technology, Inc.

DNA synthesis analysis. DNA synthesis was examined using a BrdU incorporation assay (28, 30, 34). The cells were examined using the Nikon Eclipse TE2000-E microscope at $\times 200$ magnification with the appropriate fluorescence filters to identify microinjected or transfected cells. The mitotic index was defined as the percentage of BrdU-positive microinjected or transfected cells per field divided by the total number of microinjected or transfected cells per field. A total of 200 cells were counted for each condition in each experiment.

Cell count assay. Preconfluent LAMd cells, plated on 6-well plates, were serum deprived for 24 h and then maintained for 14 days in serum-free medium, which was changed daily and supplemented with diluent, 0.3 or 0.5 μ M simvastatin, or 20 nM rapamycin alone or in combination with 0.5 μ M simvastatin. Cell counts were performed on days 0, 2, 4, 6, 8, 10, 12, and 14. A minimum of three repetitions were performed for each condition in each experiment.

Rho activation assay. Rho activity was examined using the EZ-Detect Rho activation kit (Pierce, Rockford, IL) according to the manufacturer's protocol as described previously (27, 31).

Apoptosis analysis. Apoptosis analysis of TSC2-null ELT3 cells that were serum deprived for 24 h and incubated with 0.1, 1, or 10 μ M simvastatin alone or in combination with 20 nM rapamycin, 0.2 or 2 μ g/ml C3 transferase, or diluent for 18 h was performed as described previously (29). Analysis of the apoptosis of ELT3 cells transfected with siRNA for RhoA or scrambled siRNA was performed using an Alexa Fluor Annexin V/Dead Cell Apoptosis kit (Molecular Probes, Inc., Eugene, OR) according to the manufacturer's protocol. Briefly, serum-deprived cells transfected with siRNA for RhoA or control siRNA for GLO were washed with ice-cold PBS, resuspended in annexin-binding buffer, and then incubated for 15 min with annexin V conjugate. Then, the cells were washed with annexin-binding buffer, deposited on glass slides, mounted in Vectashield mounting medium, and visualized on the Nikon Eclipse E400 microscope using the appropriate filters. Data are represented as the percentage of

apoptotic cells per total number of cells, taken as 100%. A total of 200 cells were counted for each condition in each experiment.

Tissue sections of subcutaneous tumors from NCRNU-M athymic female mice treated with diluent, simvastatin, or rapamycin or cotreated with simvastatin and rapamycin were subjected to analysis of apoptosis using the *In Situ* Cell Death Detection Kit based on terminal deoxynucleotidyltransferase-mediated dUTP-biotin nick end labeling (TUNEL) technology (Roche, Nutley, NJ) according to the manufacturer's protocol. Tumors from a minimum of five animals for each treatment condition were analyzed.

Flow cytometry analysis. *Tsc2*^{+/+} *p53*^{-/-} and *Tsc2*^{-/-} *p53*^{-/-} MEFs and isogenic *Tsc2*^{-/-} and *Tsc2*^{+/+} MEFs were maintained in serum-free medium with 1 μ g/ml C3 transferase or diluent for 18 h, and then flow cytometry analysis with primary annexin V and secondary fluorescein isothiocyanate (FITC)-conjugated antibodies was performed as we described previously (28). The negative control included diluent-treated cells incubated with matched IgG and secondary FITC-conjugated antibody.

Animals. All animal procedures were performed accordingly to a protocol approved by the University of Pennsylvania Animal Care and Use Committee (IACUC). Six- to 8-week-old NCRNU-M athymic nude female mice (Taconic) were injected subcutaneously in both flanks with 5×10^6 TSC2-null ELT3 cells (see Fig. 9A for the experimental scheme). When tumors reached 5 mm in diameter, the mice were transferred to a diet supplemented with simvastatin (250 mg/kg of body weight/day) or injected with rapamycin (intraperitoneal [i.p.] injections, 1 mg/kg 3 times a week) alone or in combination with a simvastatin diet for 50 days. These doses of simvastatin and rapamycin were chosen based on published observations (41, 48, 90). Chow containing simvastatin was prepared by Animal Specialties & Provision (Quakertown, PA) (JL Rat & Mouse/4F [5LG6] diet based on regular chow, received by the control group, and supplemented with simvastatin [Zocor; Merck]). Animals from each group were euthanized at days 0, 10, and 20 of treatment or when tumors reached 10 mm in diameter; the tumors were removed and evaluated by histological (hematoxylin and eosin [H&E]) and immunohistochemical analyses. Survival analysis was performed using the termination time, when the tumor diameter reached 10 mm. During the treatment time, the general behavior of the mice was monitored three times a week. Tumor size was monitored three times a week and measured using calipers. Tumor volumes were calculated using the following formula, as described previously (87): length \times width² \times 0.5. Mouse weight was monitored throughout the experiment, and no significant differences in weight were detected between mice receiving the simvastatin-supplemented diet and mice receiving a regular diet; the average weight of simvastatin-treated animals after 50 days of treatment was 25.488 \pm 0.407 g, and that of animals receiving a regular diet was 25.980 \pm 1.352 g. During the treatment period, 4 animals were sacrificed: 1 control mouse, 1 rapamycin-treated mouse, and 1 simvastatin-treated mouse were sacrificed due to tumor-related weight loss at days 15, 50, and 22 of treatment, respectively; 1 rapamycin-treated mouse was sacrificed at day 24 of treatment because of an open sore. While these deaths did not cluster in either the rapamycin or the simvastatin treatment groups and thus were not attributed to drug toxicity, these mice were excluded from the analysis. To determine whether rapamycin or simvastatin withdrawal induced the tumor recurrence, treatment of tumor-free animals was terminated after 50 days, and the animals were monitored three times a week; when tumors reached 10% of the animal's body weight, the animals were sacrificed.

Immunohistochemical analysis. Immunohistochemical analysis was performed using sections of tumor tissues, which were snap-frozen in OCT embedding compound (Tissue-Tek, Tokyo, Japan) as described previously (28, 29). Tissue sections were immunostained with anti-Ki-67 (Fisher Scientific International Inc., Hampton, NH) and anti-phospho-S6 (anti-P-S6) antibodies (Cell Signaling Technology, Beverly, MA). Staining with 4',6-diamidino-2-phenylindole (DAPI) was performed to detect cell nuclei. Tumors from a minimum of five animals per treatment condition were analyzed. Staining was visualized using a Nikon Eclipse TE2000-E microscope with appropriate filters. S6 phosphorylation levels were analyzed by optical density (OD) using Gel-Pro Analyzer software; the P-S6 OD at day 0 was taken as 100%, as we previously described (27, 30). Proliferation levels were determined as a percentage of Ki67-positive cells per total number of cells, taken as 100%. A minimum of 300 cells were analyzed per condition in each tumor.

Data analysis. Data points from individual assays represent mean values \pm standard errors (SE). Statistically significant differences among groups were assessed by analysis of variance (ANOVA) (Bonferroni-Dunn), with *P* values of <0.05 sufficient to reject the null hypothesis for all analyses. All experiments were designed with matched control conditions within each experiment to enable statistical comparison as paired samples.

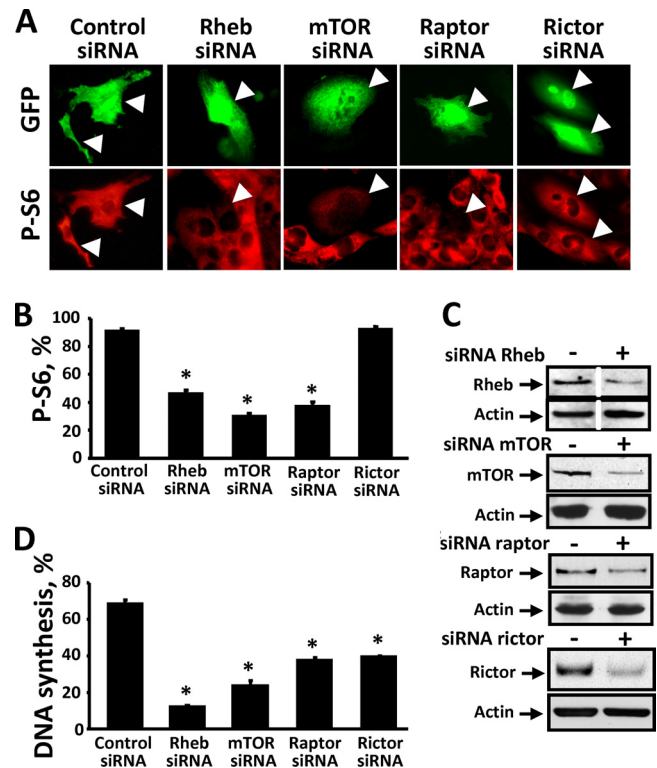


FIG. 1. (A and B) Rheb, mTOR, and raptor, but not rictor, are required for S6 phosphorylation in TSC2-null cells. (A) Cells were comicroinjected with siRNA specific to Rheb, mTOR, raptor, or rictor or control scrambled siRNA and GFP; then, dual immunocytochemical analysis was performed with phospho-S6 antibody (red) and GFP (green) to detect microinjected cells (arrowheads). (B) The data represent the percentage of P-S6-positive cells per total number of microinjected cells (mean values \pm SE) by ANOVA (Bonferroni-Dunn). *, *P* < 0.001 for control siRNA versus siRNA for Rheb, siRNA for mTOR, and siRNA for raptor. (C) TSC2-null cells were transfected with 50 ng/ml specific siRNAs (+) or scrambled control siRNA (-); 48 h posttransfection, protein levels were detected by immunoblot analysis with specific anti-Rheb, anti-mTOR, anti-rictor, and anti-raptor antibodies. The lanes separated by white lines were run on the same gel but were noncontiguous. (D) Rheb, mTOR, raptor, and rictor are required for TSC2-null cell proliferation. Cells were comicroinjected with siRNA for mTOR, siRNA for Rheb, siRNA for raptor, or siRNA for rictor or scrambled control siRNA, followed by a BrdU incorporation assay. The mitotic index represents the percentage of BrdU-positive microinjected cells compared to the total number of microinjected cells. The data represent mean values \pm SE by ANOVA (Bonferroni-Dunn). *, *P* < 0.001 for control siRNA versus Rheb, mTOR, raptor, and rictor siRNAs.

RESULTS

mTORC2 is required for TSC2-null cell proliferation. Activation of mTOR, which forms the catalytic core of multiprotein complexes mTORC1 and mTORC2, is modulated by raptor and rictor, respectively. Loss of TSC2 increases cell proliferation due to the constitutive activation of mTORC1 through the small GTPase Rheb (65), while the role of mTORC2 in TSC2-dependent cell proliferation remains unknown. We examined whether mTORC2 is required for cell proliferation due to TSC2 loss using TSC2-null ELT3 cells derived from the Eker rat uterine leiomyoma (38). As seen in Fig. 1, siRNA-induced depletion of mTOR, Rheb, and raptor

inhibited S6 phosphorylation (P-S6) (Fig. 1A and B) and TSC2-null cell proliferation (Fig. 1D) compared to control scrambled siRNA. In contrast, siRNA depletion of rictor had little effect on P-S6, confirming that mTORC2 is not involved in the constitutive activation of S6K1 signaling in TSC2-null cells (Fig. 1A and B). These data are consistent with our and other's published data (9, 30, 32, 95) showing that mTOR, Rheb, and raptor are required for TSC2-null cell proliferation. To test the direct involvement of mTORC2 signaling in cell proliferation, we compared the effects of siRNA for rictor to those of siRNA for mTOR and siRNA for raptor on TSC2-null cell proliferation. Not surprisingly, raptor and mTOR depletion inhibited cell proliferation (Fig. 1D). Importantly, siRNA for rictor also significantly inhibited TSC2-null cell DNA synthesis (Fig. 1D), demonstrating that both raptor and rictor are required for TSC2-null cell proliferation. Thus, our data show that in cells deficient in TSC2, Rheb and mTORC1, but not mTORC2, are required for the activation of S6K1 signaling. Notably, siRNA for rictor and siRNA for raptor attenuated only TSC2-null cell proliferation, suggesting that both mTORC1 and mTORC2 are required for TSC2-null cell proliferation.

mTORC2 is required for increased RhoA GTPase activity in TSC2-null cells. In both yeast and mammals, mTORC2 regulates actin stress fiber formation through regulation of RhoA GTPase (44, 75). We demonstrated that TSC2 loss upregulates RhoA activity and stress fiber formation through TSC1 and Rac1 (27, 31). Consistent with our published data (27, 31), TSC2 loss activated RhoA GTPase (Fig. 2A) that manifested as increased stress fiber formation (data not shown) and was inhibited by TSC2 reexpression (Fig. 2A).

To determine whether mTORC2 acts downstream of TSC2 in regulating RhoA activity, TSC2-null and LAMD cells were transfected with siRNA for rictor (Fig. 2B, top). As shown in Fig. 2B, cells transfected with control scrambled siRNA had marked Akt phosphorylation at Ser 473 (P-Ser473 Akt), indicating that mTORC2 is activated in TSC2-null and LAMD cells. Interestingly, in *Tsc2*^{-/-} MEFs, P-Ser473 Akt was shown to be reduced (40), suggesting that TSC2 loss could have different effects on mTORC2 activity depending on the cell type. In TSC2-null ELT3 and LAMD cells, siRNA for rictor inhibited P-Ser473 Akt compared to control siRNA but had little effect on phospho-S6 levels.

Analysis of RhoA GTPase activity demonstrated that serum-deprived TSC2-null and LAMD cells transfected with control scrambled siRNA had marked RhoA activation (Fig. 2C), as demonstrated by our published studies (27, 31). In contrast, RhoA activity was significantly downregulated in rictor siRNA-transfected cells (Fig. 2C and D), demonstrating that mTORC2 is required for RhoA GTPase activation in cells with TSC2 loss or deficiency. Surprisingly, siRNA for rictor had little effect on P-Ser2481 mTOR in TSC2-null and LAMD cells (data not shown). In contrast, in TSC2-positive rat PAVSM cells used for comparison to human smooth-muscle-like LAMD cells, siRNA for rictor decreased both P-Ser2481 mTOR and P-Ser473 Akt, while it had little effect on P-S6 (55 and data not shown). Since P-Ser2481 mTOR manifests mTOR intrinsic catalytic activity in both mTORC1 and mTORC2 (82), mTORC1 hyperactivation in TSC2-null cells may mask the effects of siRNA for rictor on P-Ser2481 mTOR

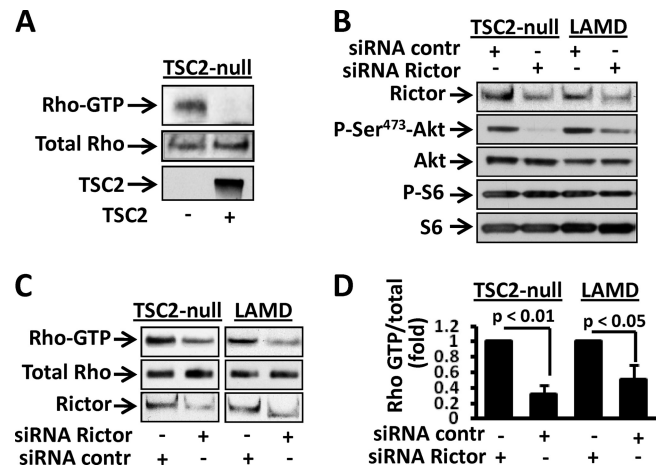


FIG. 2. (A) Reexpression of TSC2 inhibits RhoA GTPase activity in TSC2-null cells. Shown is a RhoA activation assay of serum-deprived cells transfected with GFP-TSC2 (+) or control GFP (-). Reexpression of TSC2 was confirmed by immunoblot analysis. The images are representative of three separate experiments. (B) siRNA for rictor inhibits P-Ser⁴⁷³-Akt in TSC2-null and LAMD cells. Serum-deprived cells, transfected with siRNA for rictor or control scrambled siRNA, were subjected to immunoblot analysis with specific antibodies to detect the indicated proteins. (C) siRNA for rictor inhibits RhoA activity in TSC2-null and LAMD cells. Serum-deprived cells were transfected with siRNA for rictor or control scrambled siRNA, and RhoA activity was measured using an active Rho pulldown assay followed by immunoblot analysis with anti-RhoA antibodies. Total RhoA was used as an internal control. rictor downregulation was confirmed by immunoblot analysis. (D) Statistical analysis of mTORC2-dependent inhibition of RhoA in TSC2-null and LAMD cells from two independent experiments (mean values \pm SE) by ANOVA (Bonferroni-Dunn). RhoA-GTP/total RhoA ratios for serum-deprived cells transfected with control scrambled siRNA were taken as 1-fold.

due to the experimental limitations of using siRNA in contrast to the approaches utilized in the published studies (12, 82).

RhoA is necessary for TSC2-null cell proliferation. To examine whether RhoA activation is required for increased proliferation of TSC2-null cells, we used C3 toxin, a cell-penetrating form of *Clostridium botulinum* exoenzyme that catalyzes the specific inactivation of RhoA (11). Inhibition of RhoA with C3 transferase significantly attenuated TSC2-null cell proliferation (Fig. 3A). C3 also inhibited the proliferation of primary human LAMD cells (Fig. 3B), which have increased RhoA activity (31). To directly address the role of RhoA in increased proliferation of TSC2-null cells, RhoA was downregulated with specific siRNA, followed by DNA synthesis analysis. Immunoblot analysis showed that endogenous levels of RhoA were reduced by 67 to 68% at 48 and 72 h posttransfection (Fig. 3C). The BrdU incorporation assay also showed that siRNA for RhoA had a modest but significant inhibitory effect in both TSC2-null and LAMD cells (Fig. 3D). In these experiments, DNA synthesis was measured in all cells, including both cells transfected with siRNA for RhoA and untransfected cells. This limitation of the experimental approach may account for the modest inhibitory effect of siRNA for RhoA on DNA synthesis in TSC2-null and LAMD cells. Interestingly, pharmacological inhibition of the Rho-associated kinase (ROCK), an established downstream effector of RhoA GTPase (16), with its specific inhibitor HA1077 reduced TSC2-

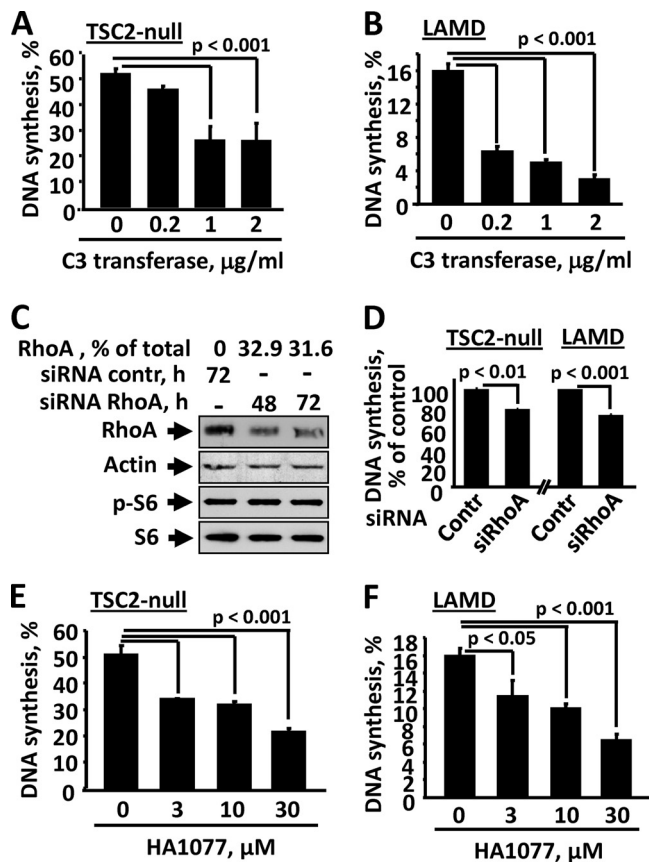


FIG. 3. (A to D) RhoA GTPase contributes to TSC2-null and LAMD cell proliferation. (A and B) C3 transferase inhibits DNA synthesis in TSC2-null and LAMD cells. Serum-deprived TSC2-null (A) or primary human LAMD (B) cells were incubated with different concentrations of C3 transferase or diluent for 18 h, followed by DNA synthesis analysis using a BrdU incorporation assay. The data represent the percentage of BrdU-positive cells per total number of cells (mean values and SE by ANOVA [Bonferroni-Dunn]); 200 cells per condition were analyzed in each experiment. (C) TSC2-null cells were transfected with siRNA for RhoA or control (scrambled) siRNA (contr) and serum deprived, and then immunoblot analysis with anti-RhoA, anti-total actin, anti-phospho-S6, and anti-total S6 antibodies was performed. (D) siRNA for RhoA inhibits TSC2-null and LAMD cell proliferation. Serum-deprived cells were transfected with siRNA for RhoA or control siRNA for 72 h, followed by DNA synthesis analysis using a BrdU incorporation assay. DNA synthesis in cells transfected with control siRNA was taken as 100%. The data represent mean values \pm SE from three independent experiments by ANOVA (Bonferroni-Dunn); 200 cells per condition were analyzed in each experiment. (E and F) HA1077 attenuates TSC2-null and LAMD cell proliferation. Serum-deprived TSC2-null ELT3 (E) and LAMD (F) cells were incubated with diluent or different concentrations of HA1077 for 18 h, followed by DNA synthesis analysis using the BrdU incorporation assay. The data represent the percentage of BrdU-positive cells per total number of cells (mean values \pm SE by ANOVA [Bonferroni-Dunn]); 200 cells per condition were analyzed in each experiment.

null and LAMD cell proliferation in a concentration-dependent manner (Fig. 3E and F, respectively), demonstrating that RhoA and its downstream effector ROCK contribute to the increased proliferation of TSC2-null and LAMD cells.

Collectively, our data demonstrate that increased proliferation of cells with TSC2 loss or dysfunction is, in part, due to

RhoA activation. Notably, siRNA for RhoA and C3 transferase attenuated DNA synthesis, and siRNA-dependent depletion of RhoA had little effect on mTORC1 activity, as shown by the unchanged S6 phosphorylation levels (Fig. 3C), suggesting that RhoA and mTORC1 act in parallel to promote TSC2-null cell proliferation.

Since mTORC2 is required for TSC2-null cell proliferation (Fig. 1D) and RhoA is downstream of mTORC2 (Fig. 2C and D), we next determined whether mTORC2 modulates TSC2-null cell proliferation via RhoA. TSC2-null cells were coinjected with siRNA for rictor and the constitutively active RhoA mutant GST-V14RhoA or control GST plasmids, and then DNA synthesis was assessed using a BrdU incorporation assay. As shown in Fig. 4A, siRNA for rictor markedly inhibited DNA synthesis in TSC2-null cells; importantly, activated V14RhoA rescued rictor siRNA-induced inhibition of DNA synthesis. These data demonstrate that RhoA acts downstream of mTORC2 in modulating TSC2-null cell proliferation. Interestingly, we also found that V14RhoA only partially reversed TSC2-induced inhibition of DNA synthesis due to reexpression of TSC2 or siRNA-induced downregulation of TSC1 (Fig. 4B and C). This evidence and our data showing that either siRNA for rictor or siRNA for raptor alone only partially inhibits DNA synthesis in TSC2-null cells (Fig. 1D) suggest that both mTORC2 and mTORC1 are necessary to rescue growth inhibition induced by TSC2 reexpression.

RhoA GTPase is required for TSC2-null cell survival. Because RhoA GTPase modulates cell survival in some cell types (74) and because of the modest inhibitory effect of siRNA for RhoA on TSC2-null cell proliferation, we examined whether RhoA is required for the survival of TSC2-null cells. Using two complementary approaches, depletion of endogenous RhoA with specific siRNA (Fig. 3C) and specific inhibition of RhoA activity with C3 transferase, we examined TSC2-null cell apoptosis. Analysis of apoptosis with an Alexa Fluor Annexin V/Dead Cell Apoptosis kit demonstrated that control (scrambled) siRNA had little effect on cell apoptosis (Fig. 5A). In contrast, siRNA for RhoA markedly promoted apoptosis at 48 h and 72 h of transfection (Fig. 5A). Inhibition of RhoA GTPase activity with C3 transferase also promoted apoptosis of TSC2-null cells in a concentration-dependent manner (Fig. 5B). Interestingly, HA1077-dependent inhibition of ROCK, while inhibiting cell proliferation (Fig. 3E), had little effect on apoptosis in TSC2-null cells (data not shown), suggesting that downregulation of RhoA induces apoptosis in a ROCK-independent manner. Taken together, these data demonstrate that downregulation of RhoA protein levels or activity induces apoptosis and suggest that RhoA activity is required for TSC2-null cell survival.

Studies demonstrate that RhoA GTPase may regulate cell survival via Bcl2 family proteins in a p53-independent manner (13, 19, 26). We next, examined whether suppression of RhoA activity with C3 transferase modulates the levels and/or phosphorylation of Bcl2 family proteins in TSC2-null and LAMD cells. As shown in Fig. 5C, inhibition of RhoA GTPase in TSC2-null ELT3 cells markedly reduced levels of the prosurvival protein Bcl2 and increased the levels of the proapoptotic BH3-only proteins Bim and Bok. In LAMD cells, inhibition of RhoA activity also decreased Bcl2 protein levels while increasing proapoptotic Bim and Puma protein levels (Fig. 5D). In-

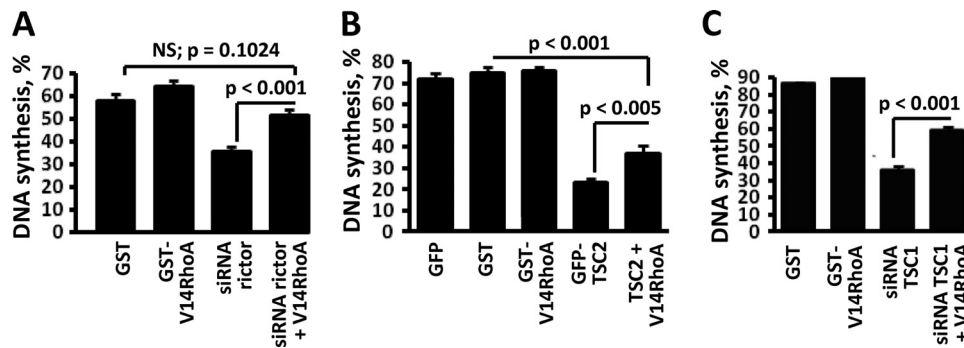


FIG. 4. Constitutively active RhoA GTPase rescues rictor siRNA, TSC2-, and TSC1-siRNA induced inhibition of DNA synthesis in TSC2-null cells. Cells were transfected with siRNA for rictor (A), GFP-TSC2 (B), and siRNA for TSC1 (C) alone or in combination with constitutively active RhoA mutant GST-V14RhoA. GFP and GST plasmids were used as controls. Then, the cells were serum deprived for 24 h, followed by DNA synthesis analysis using the BrdU incorporation assay. The data represent the percentage of BrdU-positive cells per total number of cells (taken as 100%). The data are mean values \pm SE from two independent experiments by ANOVA (Bonferroni-Dunn). A minimum of 200 cells per condition were counted in each experiment.

terestingly, C3 transferase had little effect on the phosphorylation of Bad in both TSC2-null and LAMD cells. Importantly, Bok, which is expressed predominantly in reproductive tissues (39), was increased in TSC2-null ELT3 cells, which are derived from rat uterine leiomyomas, suggesting that RhoA-dependent apoptosis can be cell type specific. Notably, inhibition of RhoA had little effect on mTORC1-dependent P-S6 and mTORC2-dependent P-Ser473 Akt, suggesting that RhoA acts downstream of mTORC2 in modulating Bcl2 family protein levels, potentially in parallel with mTORC2-Akt signaling. Taken together, these data demonstrate that RhoA GTPase modulates the survival of cells with TSC2 loss and deficiency via Bcl2 family proteins.

To determine whether p53 is involved in RhoA-dependent modulation of TSC2-null cell survival, we performed immunoblot analysis of LAMD cells treated with C3 transferase with phospho-Ser46 p53 (P-Ser46 p53) antibody and found that inhibition of RhoA GTPase had little effect on P-p53 and p53 protein levels (data not shown). Next, we examined C3 transferase-induced apoptosis in *Tsc2*^{-/-} and *Tsc2*^{+/+} MEFs compared to *Tsc2*^{-/-} *p53*^{-/-} and *TSC2*^{+/+} *p53*^{-/-} MEFs with p53 deleted (94) using flow cytometry analysis with annexin V antibody. We found that all diluent-treated cells had low levels of apoptosis (Fig. 5E). Inhibition of RhoA increased apoptosis by 15 to 20% in *Tsc2*^{-/-} and *Tsc2*^{+/+} MEFs at levels comparable to those of *Tsc2*^{+/+} *p53*^{-/-} MEFs (Fig. 5E), suggesting that either TSC2 or p53 loss alone has little effect on basal and C3 transferase-induced apoptosis. In contrast, inhibition of RhoA in *Tsc2*^{-/-} *p53*^{-/-} MEFs markedly increased apoptosis compared to *Tsc2*^{-/-}, *Tsc2*^{+/+}, and *Tsc2*^{+/+} *p53*^{-/-} MEFs (Fig. 5E), demonstrating that loss of both TSC2 and p53 augments cell sensitivity to RhoA inhibition. These data suggest that p53 is necessary for RhoA-dependent *Tsc2*^{-/-} *p53*^{-/-} MEF survival but that these effects maybe cell type specific.

Simvastatin inhibits RhoA GTPase activity and the proliferation of TSC2-null cells. Simvastatin inhibits proliferation and induces apoptosis in different cell types through inhibition of RhoA GTPase activity by preventing RhoA geranylgeranylation (4, 23, 84). To directly examine the effect of simvastatin on RhoA GTPase activity, we performed a RhoA activation assay in TSC2-null and LAMD cells treated with different

concentrations of simvastatin. As seen in Fig. 6A and B, respectively, simvastatin inhibited RhoA GTPase activity in TSC2-null and primary human LAMD cells in a concentration-dependent manner. Because RhoA activity is required for cell migration and to confirm that simvastatin-dependent RhoA inhibition is functionally significant for LAMD cells, the migration assay was performed under the same experimental conditions. We found that simvastatin inhibited LAMD cell migration in a concentration-dependent manner that correlated with its effects on RhoA activity (data not shown). Since simvastatin inhibits proliferation in different types of cells, including cancer and smooth muscle cells (1, 4, 7), and our data show that RhoA is required for TSC2-null cell proliferation (Fig. 3), we examined the effects of simvastatin alone and in combination with rapamycin on the proliferation of TSC2-null and LAMD cells that were treated with different concentrations of simvastatin, 20 nM rapamycin, or diluent separately or in combination. As shown in Fig. 7A, simvastatin inhibited DNA synthesis in TSC2-null cells in a concentration-dependent manner. In agreement with our previous studies (28), 20 nM rapamycin alone markedly inhibited the DNA synthesis. Combined treatment with simvastatin and rapamycin further inhibited DNA synthesis of TSC2-null cells compared to treatment with rapamycin alone (Fig. 7A, black bars). Similarly, in primary human LAMD cells, simvastatin alone attenuated DNA synthesis in a concentration-dependent manner and markedly enhanced the growth-inhibitory effect of rapamycin (Fig. 7B). Similar results were obtained using cell counts: LAMD cell growth in the presence of 0.3 and 0.5 μ M simvastatin was markedly attenuated in a concentration-dependent manner compared to diluent-treated cells (Fig. 7C). Maintenance in media supplemented with 20 nM rapamycin inhibited LAMD cell growth, and simvastatin-rapamycin cotreatment significantly enhanced the inhibitory effects of either rapamycin or simvastatin given separately (Fig. 7D). Taken together, these data demonstrate that simvastatin alone attenuates TSC2-null and LAMD cell proliferation and cooperates with rapamycin in the inhibition of cell growth caused by TSC2 loss or dysfunction.

Simvastatin promotes apoptosis in TSC2-null cells via RhoA GTPase. Next, we examined whether simvastatin pro-

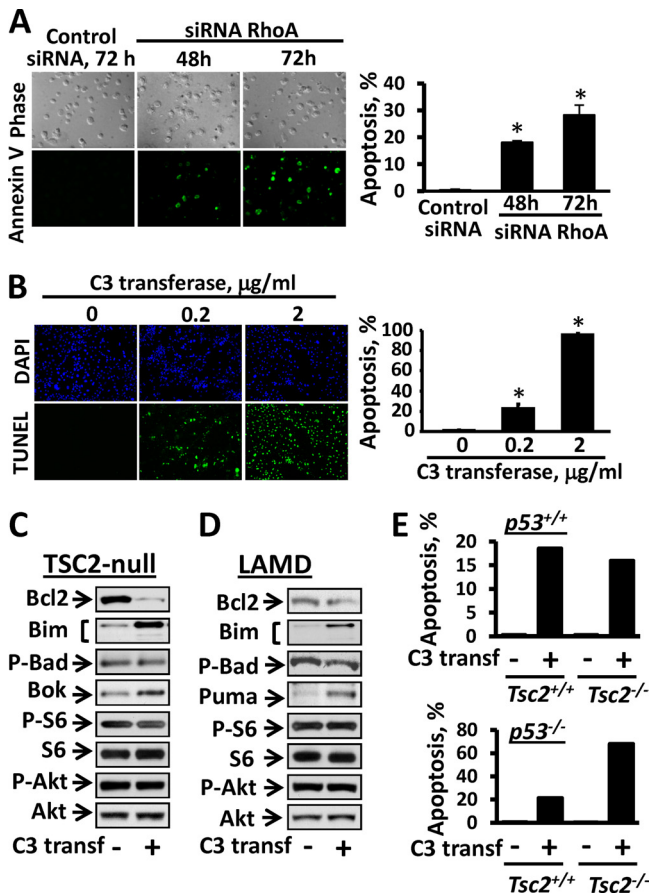


FIG. 5. (A) RhoA is required for TSC2-null cell survival. Cells transfected with control (scrambled) or RhoA for siRNA for 48 and 72 h were resuspended in annexin V binding buffer, incubated with annexin V conjugate, and then plated on glass slides. Apoptotic cells were visualized using an Eclipse E400 microscope under $\times 200$ magnification with appropriate filters. (Left) Representative images of three independent experiments. (Right) Statistical analysis. The data represent the percentage of apoptotic cells per total number of cells (taken as 100%) (mean values \pm SE from three independent repetitions). A minimum of 200 cells were analyzed per experimental condition. *, $P < 0.001$ for siRNA for RhoA versus control siRNA by ANOVA (Bonferroni-Dunn). (B) C3 transferase promotes apoptosis in TSC2-null cells. (Left) Serum-deprived cells were incubated with different concentrations of C3 transferase or diluent for 18 h, followed by apoptosis analysis using the *In Situ* Cell Death Detection kit. (Right) The data represent the percentage of apoptotic cells per total number of cells (taken as 100%); 200 cells per condition were analyzed in each experiment. The data are mean values and SE. *, $P < 0.001$ for C3 transferase versus diluent by ANOVA (Bonferroni-Dunn). (C and D) C3 transferase modulates levels of Bcl2 family proteins. Serum-deprived TSC2-null (C) and LAMD (D) cells were treated with 1 μ g/ml C3 transferase (C3 transf) (+) or diluent (-), followed by immunoblot analysis with specific antibodies to detect the indicated proteins. The images are representative of two separate experiments. (E) *Tsc2*^{+/+} and *Tsc2*^{-/-} MEFs with p53 (top) and *Tsc2*^{+/+} *p53*^{-/-} and *Tsc2*^{-/-} *p53*^{-/-} MEFs with p53 deleted (bottom) were maintained in serum-free medium with 1 μ g/ml C3 transferase (+) or diluent (-) for 18 h, and then flow cytometry analysis with primary annexin V and secondary FITC-conjugated antibodies was performed. The negative control included diluent-treated cells incubated with matched IgG and secondary FITC-conjugated antibody. The data represent the percentage of annexin V-positive cells per total number of cells.

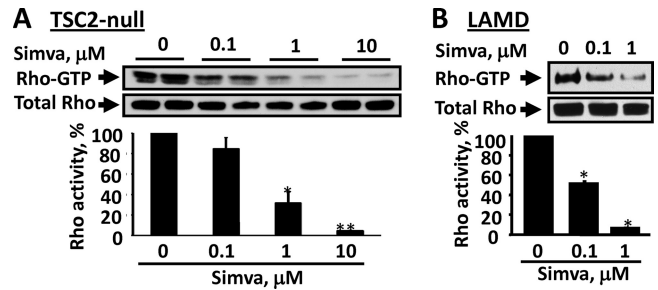


FIG. 6. Simvastatin inhibits RhoA GTPase activity. Serum-deprived TSC2-null (A) and LAMD (B) cells were treated with the indicated concentrations of simvastatin (Simva) or diluent, followed by Rho activation assay. (Top) RhoA-GTP was pulled down with Rho-tekkin-RBD agarose, followed by immunoblot analysis with anti-RhoA antibodies. Total RhoA was used as an internal control. The images are representative of two independent experiments. (Bottom) Statistical analysis of experiments. The data represent mean values \pm SE from two independent experiments. (A) *, $P < 0.05$ for 1 μ M simvastatin versus diluent; **, $P < 0.001$ for 10 μ M simvastatin versus diluent. (B) *, $P < 0.001$ for simvastatin versus diluent by ANOVA (Bonferroni-Dunn).

promotes apoptosis in TSC2-null cells, since our data demonstrate that RhoA is required for TSC2-null cell survival (Fig. 5) and that simvastatin inhibits RhoA activation (Fig. 6). As shown in Fig. 8A and B, simvastatin induced apoptosis in TSC2-null cells in a concentration-dependent manner. Rapamycin, as we reported previously (29), had little effect on the number of apoptotic cells compared to diluent-treated cells (Fig. 8B). Interestingly, cotreatment with rapamycin modestly increased simvastatin-induced apoptosis (Fig. 8B). These data demonstrate that simvastatin induces apoptosis in TSC2-null cells.

To determine whether simvastatin promotes apoptosis by inhibiting RhoA GTPase, we transfected TSC2-null cells with constitutively active V14RhoA, and then the cells were treated with simvastatin, followed by assessment of cell apoptosis using immunostaining with cleaved caspase 3 antibody. As seen in Fig. 8C and D, simvastatin promoted a marked increase in cleaved caspase 3 immunostaining. Importantly, cells transfected with constitutively activated V14RhoA stained negative for cleaved caspase 3 antibody, demonstrating that activated RhoA rescues simvastatin-induced apoptosis in TSC2-null cells (Fig. 8D). Collectively, these data suggest that simvastatin induces apoptosis via inhibition of RhoA GTPase through cleavage of caspase 3 in TSC2-null cells.

Simvastatin and rapamycin inhibit TSC2-null tumor growth in nude mice and improve the survival of tumor-bearing mice. To examine whether our *in vitro* findings have *in vivo* relevance, we examined the effects of simvastatin alone or in combination with low-dose rapamycin on xenographic TSC2-null tumor growth in nude mice. NCRNU-M athymic nude mice were injected subcutaneously with 5×10^6 TSC2-null ELT3 cells. Tumors reached 5 mm in diameter in 4 to 6 weeks; then, the animals were treated with simvastatin (250 mg/kg/day; special diet), rapamycin (1 mg/kg; i.p. injections 3 times a week), or a combination of simvastatin and rapamycin for 50 days. A schematic representation of the experimental design is shown in Fig. 9A. The dose levels and treatment schedule for rapamycin were selected on the basis of previously verified pharmacokinetics and the doses of rapamycin approved for immu-

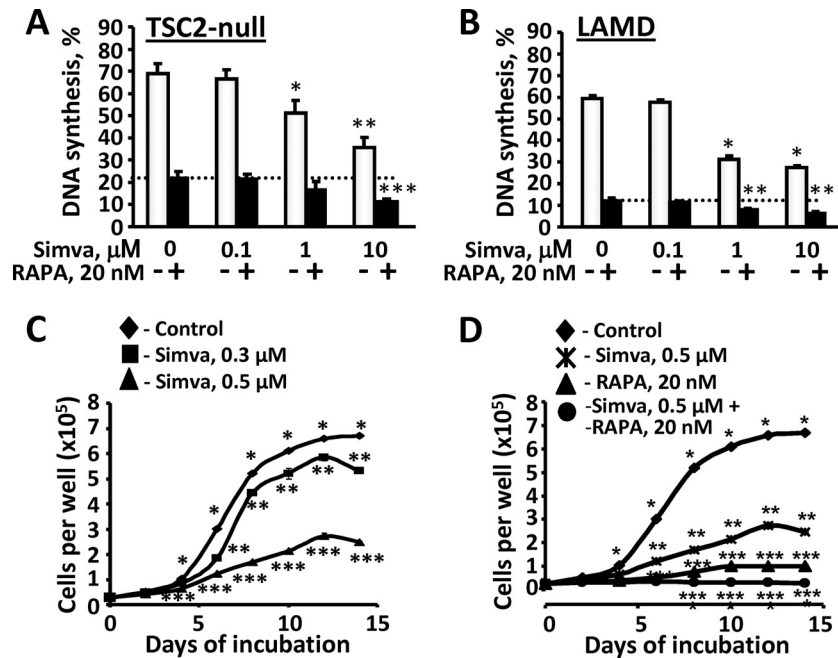


FIG. 7. (A and B) Effects of simvastatin and rapamycin on DNA synthesis in TSC2-null and LAMD cells. TSC2-null (A) and LAMD (B) cells serum deprived for 24 h were treated with the indicated concentrations of simvastatin (Simva) or diluent alone or in the presence of 20 nM rapamycin (RAPA) for 18 h, followed by DNA synthesis analysis using the BrdU incorporation assay. The data represent the percentage of BrdU-positive cells per total number of cells (mean values \pm SE from three independent experiments). A minimum of 200 cells were analyzed per condition in each experiment. (A) *, $P < 0.05$ for 1 μM simvastatin versus diluent; **, $P < 0.001$ for 10 μM simvastatin versus diluent; ***, $P < 0.001$ for simvastatin plus RAPA versus RAPA. (B) *, $P < 0.001$ for simvastatin versus diluent; **, $P < 0.01$ for simvastatin plus RAPA versus RAPA by ANOVA (Bonferroni-Dunn). (C and D) Simvastatin and rapamycin inhibit LAMD cell growth. Serum deprived for 24 h, cells were maintained for 14 days in serum-free medium containing the indicated concentrations of simvastatin (Simva) or diluent (C) or 0.5 μM simvastatin and 20 nM RAPA separately or in combination (D) that was changed daily. Cell counts were performed every second day with three repetitions for each condition. (C) *, $P < 0.001$ for diluent-treated cells on day 0 versus diluent-treated cells on days 2 to 14; **, $P < 0.01$ for 0.3 μM simvastatin versus diluent; ***, $P < 0.001$ for 0.5 μM simvastatin versus diluent. (D) *, $P < 0.001$ for diluent-treated cells on day 0 versus diluent-treated cells on days 2 to 14; **, $P < 0.001$ for simvastatin versus diluent; ***, $P < 0.001$ for RAPA versus diluent; ****, $P < 0.01$ for simvastatin plus RAPA versus simvastatin and for simvastatin plus RAPA versus RAPA by ANOVA (Bonferroni-Dunn).

nosuppression after organ transplantation (67), clinical trials (3), and dose-response rodent studies (41). Notably, the doses of rapamycin used in this study were 4 to 10 times lower than those in previous reports (59–61, 68, 72). The treatment dose and administration for simvastatin were selected based on published studies as the highest well-tolerated dose that had also shown biological activity in rodent models (48, 79, 90). No significant changes in general behavior and weight were observed during the treatment period and after treatment was terminated (animal weight by day 50 of the experiment was 25.49 ± 0.41 g for simvastatin-treated animals and 25.98 ± 1.35 g for animals on a regular diet). To determine the effects of simvastatin and rapamycin on TSC2-null tumor growth, tumor size was monitored three times a week by measurement with calipers. Animals were sacrificed when the tumors reached 10 mm in diameter; the date of sacrifice was also used as the date of termination for survival analysis.

Analysis of tumor-bearing mouse survival demonstrated that only 15% of control animals survived by day 50 of the experiment (Fig. 9B). Simvastatin and rapamycin used alone increased animal survival by 47.64% and 50.0%, respectively (Fig. 9B). Importantly, combined treatment with rapamycin and simvastatin markedly improved survival compared to animals treated with simvastatin and rapamycin singly. Thus, after

50 days of combined treatment, animal survival was 67.0%, which was more than 4 times higher than the control group (Fig. 9B).

Analysis of TSC2-null tumor growth demonstrated marked tumor growth in control (untreated) mice. Thus, tumor volumes doubled by day 6 and showed an approximately 3-fold increase by day 13 from the beginning of the experiment (Fig. 9C). During the first 40 days of treatment, rapamycin and simvastatin had marked inhibitory effects on tumor growth compared to control animals, showing an approximately 3.5-fold increase in tumor volume during the same period (Table 1). The combination of simvastatin and rapamycin reduced tumor volume by 4 weeks of treatment. Interestingly, both simvastatin and rapamycin as single agents abrogated tumor growth at approximately day 45 (Fig. 9C).

Taken together, these data demonstrate that rapamycin and simvastatin alone inhibited TSC2-null tumor growth in nude mice and increased animal survival and that combined treatment with simvastatin and rapamycin abrogated tumor growth and improved animal survival compared to control and single-agent treatments.

Tumor recurrence in rapamycin-treated, but not simvastatin-treated, mice. To examine the effects of rapamycin and simvastatin withdrawal on TSC2-null tumor growth, mice that

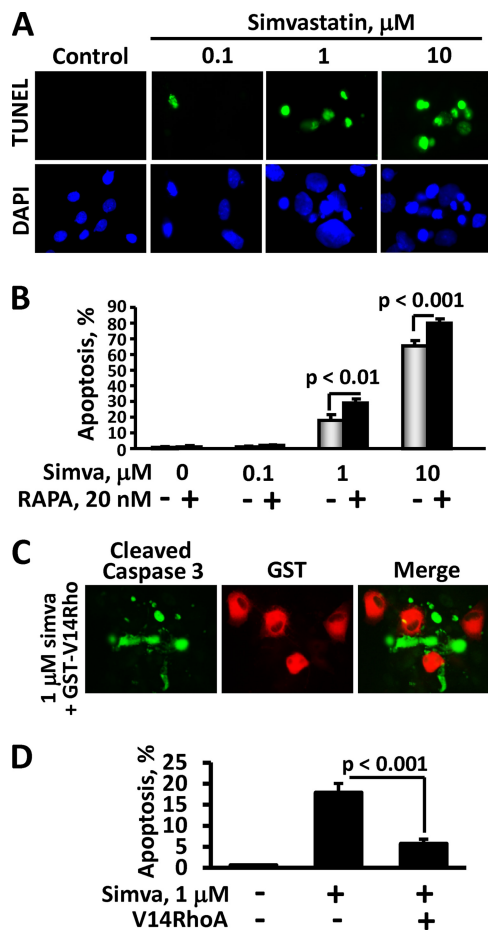


FIG. 8. (A and B) Simvastatin induces apoptosis in TSC2-null cells. Serum-deprived cells were treated with 0.1, 1, and 10 μM simvastatin (Simva) or diluent in the presence or absence of 20 nM rapamycin (RAPA) for 24 h, followed by apoptosis analysis using the *In Situ* Cell Death Detection Kit. (A) Representative images from three independent experiments were taken using an Eclipse TE2000-E microscope at $\times 400$ magnification with appropriate filters. (B) Statistical analysis. The data represent the percentage of apoptotic cells per total number of cells (taken as 100%) (mean values \pm SE from three independent experiments by ANOVA [Bonferroni-Dunn]). A minimum of 200 cells were analyzed per condition in each experiment. (C and D) Activated RhoA rescues simvastatin-induced apoptosis in TSC2-null cells. (C) Cells were transfected with GST-V14RhoA or mock transfected and treated with 1 μM simvastatin or diluent, and then dual immunocytochemical analysis to detect cleaved caspase 3 and GST was performed. (D) The data represent mean values \pm SE by ANOVA (Bonferroni-Dunn). A minimum of 200 cells were examined per condition in each experiment.

were treated with rapamycin and simvastatin separately or in combination for 50 days as described above and had visible tumor disappearance (5 animals per treatment condition) were subjected to treatment withdrawal and were monitored three times a week. Three of five animals from the rapamycin-treated group demonstrated flank tumor recurrence after treatment withdrawal. Initial tumor recurrence was observed within a week after final rapamycin administration, and during the next 41 days, tumors reached 10% of animal body weight (Fig. 9D and E). Importantly, no tumor recurrence was detected in simvastatin- and simvastatin-rapamycin-treated ani-

mals during the 9 months after treatment withdrawal (Fig. 9D and E). Collectively, these data demonstrate that the combination of rapamycin with simvastatin prevents tumor regrowth after treatment withdrawal.

Simvastatin promotes apoptosis and, in combination with rapamycin, abrogates tumor cell growth *in vivo*. Because our *in vitro* data demonstrate that simvastatin promotes apoptosis in TSC2-null ELT3 and LAMD cells, we performed apoptosis analysis of tumor tissues collected at days 0, 10, and 20 of treatment using a TUNEL-based *In Situ* Cell Death Detection Kit. As seen in Fig. 10A and B, little apoptosis was detected in control and rapamycin-treated tumors. In contrast, marked apoptosis was detected in the simvastatin- and simvastatin-rapamycin-treated tumors at days 10 and 20 of treatment (Fig. 10A and B). Similarly, marked apoptosis was detected in simvastatin- and simvastatin-rapamycin-treated tumors at days 34 and 32 of treatment, respectively, while tumors from mice treated with rapamycin alone for 41 days had low levels of apoptosis that were comparable to those of untreated tumors collected at day 45 of the experiment (Fig. 11). Taken together, these data demonstrate that simvastatin promotes apoptosis in TSC2-null tumors.

To examine the effects of simvastatin and rapamycin on TSC2-null cell growth *in vivo*, proliferation of TSC2-null cells within tumors was examined by immunohistochemical analysis with anti-Ki-67 antibodies. As shown in Fig. 10C and D and 11, tumor tissues of control animals had marked proliferation rates, which persisted to days 10, 20, and 45 of the experiment. At day 10 of treatment, rapamycin significantly inhibited cell proliferation, while simvastatin had little effect. At day 20, however, both simvastatin and rapamycin inhibited tumor cell growth (Fig. 10C and D). Importantly, combined treatment of simvastatin with rapamycin markedly reduced proliferation in a time-dependent manner compared to rapamycin or simvastatin treatment alone (Fig. 10C and D). Our data demonstrate that simvastatin and rapamycin cooperate in inhibiting the proliferation of TSC2-null cells *in vivo*.

Because rapamycin inhibits mTORC1 activity in different cell and animal models, we examined the activation state of mTORC1 by the phosphorylation levels of ribosomal protein S6, the molecular marker of mTORC1 activation, using two different techniques, immunocytochemistry and immunoblot analysis. Analysis of tumor sections with P-S6 antibodies demonstrated that TSC2-null tumors had marked P-S6 levels prior to treatment (day 0) and control (untreated) tumors maintained high P-S6 levels through days 1, 10, 20, and 45 of the experiment (Fig. 11 and 12A and B). A low dose of rapamycin (1 mg/kg) induced a marked reduction in P-S6 compared to untreated tumors in a time-dependent manner (Fig. 11 and 12). Simvastatin alone had little effect on P-S6 and did not modulate the rapamycin-dependent inhibition of P-S6 in co-treated tumors (Fig. 11 and 12). Immunoblot analysis performed using tissue samples collected at days 15, 30, and 40 of the experiment also demonstrated a marked increase in P-S6 in control tumors at days 15 and 30 (Fig. 12C). Consistent with immunohistochemical data, rapamycin decreased P-S6 at days 15, 30, and 40; simvastatin had little effect on P-S6; and combined rapamycin- and rapamycin-simvastatin-treated tumors showed decreases in P-S6 comparable to those of tumors treated with rapamycin alone (Fig. 12C and D, left). These

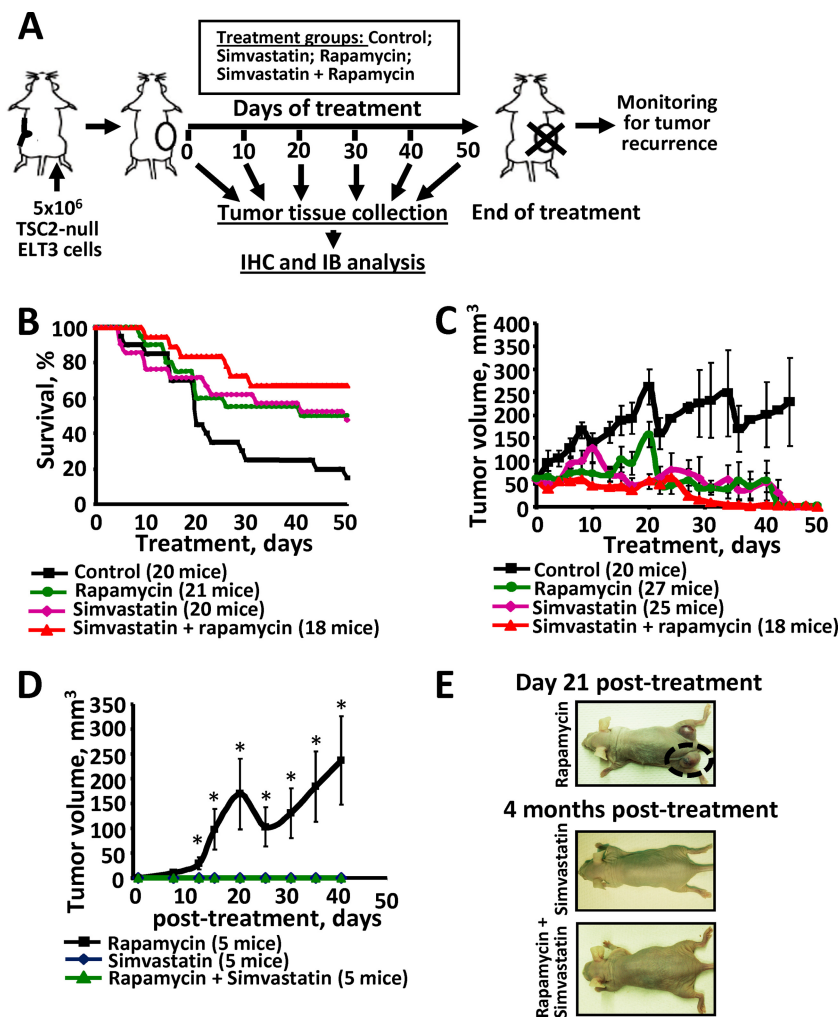


FIG. 9. (A) Schematic representation of the experimental design. NCRNU-M female athymic nude mice with TSC2-null ELT3 subcutaneous tumors were subjected to a 50-day treatment with rapamycin, simvastatin, and the combination of rapamycin and simvastatin. Untreated animals were used as controls. Upon treatment termination, mice were monitored for tumor recurrence either until the tumors reached 10% of the animal's body weight or for 9 months after treatment withdrawal. IHC, immunohistochemical; IB, immunoblotting. (B) Rapamycin and simvastatin improve the survival of mice bearing TSC2-null tumors. Survival analysis was performed using as the termination time the time when the tumor diameter reached 10 mm. Untreated mice were used as controls. A minimum of 18 mice were analyzed per experimental condition. (C) Effects of simvastatin and rapamycin on TSC2-null tumor growth in nude mice. Mice were treated as described above, and tumor growth was monitored using calipers. The data represent mean values \pm SE by ANOVA (Bonferroni-Dunn). (D and E) Simvastatin prevents posttreatment tumor regrowth. After 50 days of treatment with simvastatin and rapamycin separately or in combination, five mice from each group with visible tumor disappearance were subjected to treatment withdrawal; the animals were monitored for tumor recurrence for 9 months or until the tumors reached 10% of total body weight. (D) The data represent mean values \pm SE. *, $P < 0.01$ for rapamycin-pretreated mice versus simvastatin- or simvastatin-rapamycin-pretreated mice by ANOVA (Bonferroni-Dunn). (E) Representative images of mice at day 21 (top) and 4 months (bottom) after rapamycin and rapamycin-simvastatin treatment withdrawal. The circle indicates the recurrent tumor in the rapamycin-pretreated mouse.

data demonstrate that rapamycin, but not simvastatin, inhibits mTORC1 signaling in TSC2-null tumors.

Since simvastatin may promote apoptosis in an Akt-dependent manner (25, 42, 52), we examined P-Ser473 Akt in tumor tissue samples. As shown in Fig. 12C, P-Ser473 Akt was detected in control untreated tumors, which correlates with Akt activation *in vitro* (Fig. 2B). In agreement with previously published studies (5, 83), rapamycin increased P-Ser473 Akt in both rapamycin and rapamycin-simvastatin-treated tumors (Fig. 12C and D, right). Levels of P-Ser473 Akt in simvastatin-treated tumors, however, were comparable to those in control tumors (Fig. 12C and D, right), demonstrating that simvastatin

has little effect on P-Ser473 Akt. These data suggest that the growth-inhibitory and proapoptotic effects of simvastatin are likely Akt independent.

In summary, these data collectively demonstrate that simvastatin and rapamycin inhibit TSC2-null tumor growth through different signaling mechanisms. Rapamycin inhibits cell proliferation through the suppression of mTORC1 signaling but has little effect on apoptosis; simvastatin inhibits TSC2-null cell proliferation and induces apoptosis but has little effect on mTORC1 activity. Importantly, combined treatment with simvastatin and rapamycin induces apoptosis, abrogates proliferation, inhibits mTORC1 signaling in TSC2-null tumors, abro-

TABLE 1. Effects of simvastatin and rapamycin on TSC2-null tumor volume

| Experimental conditions (no. of animals) | Tumor volume \pm SE (mm ³) at day: | | | | |
|---|--|------------------------------|------------------------------|------------------------------|------------------------------|
| | 0 | 10 | 22 | 31 | 41 |
| 1. Control (20) | 56.1 \pm 8.6 | 141.2 \pm 18.5 | 159.7 \pm 34.4 | 232.0 \pm 81 | 201.0 \pm 71 |
| 2. Rapamycin (27) | 61.5 \pm 9.4 | 71.8 \pm 25.2 ^a | 46.5 \pm 18.4 ^a | 43.3 \pm 12.5 ^a | 57.7 \pm 43.1 ^a |
| 3. Simvastatin (25) | 57 \pm 4.4 | 128 \pm 32.8 | 64.5 \pm 23.8 ^a | 41.8 \pm 15 ^a | 53.1 \pm 21.3 ^a |
| 4. Rapamycin plus simvastatin (18) | 56.8 \pm 3.4 | 46 \pm 4.0 ^b | 48.9 \pm 16.9 ^a | 10.2 \pm 3.6 ^c | 3.6 \pm 1.9 ^b |

^a $P < 0.05$ for rapamycin and/or simvastatin versus control by ANOVA (Bonferroni-Dunn).

^b $P < 0.01$ for rapamycin plus simvastatin (day 10) versus simvastatin (day 10); for rapamycin plus simvastatin (day 41) versus rapamycin (day 41); and for rapamycin plus simvastatin (day 41) versus simvastatin (day 41) by ANOVA (Bonferroni-Dunn).

^c $P < 0.05$ for rapamycin plus simvastatin (day 31) versus rapamycin (day 31) and for rapamycin plus simvastatin (day 31) versus simvastatin (day 31) by ANOVA (Bonferroni-Dunn).

gates TSC2-null tumor growth, and prevents tumor recurrence after simvastatin and rapamycin withdrawal.

DISCUSSION

Increased proliferation of atypical smooth muscle cells in pulmonary LAM and in kidney tumors in TS occurs due to mutational inactivation of tumor suppressor *TSC2* and mTORC1 activation (54). This study demonstrates that TSC2-dependent increased cell proliferation and survival also requires mTORC2 and its downstream effector RhoA GTPase. Thus, inhibition of mTORC1 and mTORC2 signaling with siRNAs for raptor and rictor, respectively, had comparable inhibitory effects on TSC2-null cell growth, demonstrating that both mTORC1 and mTORC2 are required for TSC2-null cell proliferation. Importantly, siRNA for rictor inhibited both increased P-Ser473 Akt and RhoA activity, demonstrating mTORC2-dependent regulation of Akt and RhoA GTPase in TSC2-null and LAM cells. We also show that RhoA activity is necessary for TSC2-null cell survival and that inhibition of RhoA promotes apoptosis through downregulation of Bcl2 and upregulation of the proapoptotic proteins Bim, Bok, and Puma. *In vivo*, the combination of the proapoptotic activity of simvastatin with the cytostatic effect of rapamycin abrogated xenographic TSC2-null tumor growth in nude mice, improved animal survival, and prevented tumor recurrence after treatment withdrawal.

While the critical role of mTORC1 signaling in TSC2-deficient cell and tumor growth makes it a logical therapeutic target for LAM and TS, recent preclinical and clinical studies have demonstrated that the mTORC1 inhibitor rapamycin and its analogs have a primarily cytostatic effect in TSC2-deficient cells and tumors and that termination of treatment results in disease reversal (3, 72). Thus, data from rapamycin (sirolimus) clinical trials for patients with pulmonary LAM and TS (3, 14) show marked regression in renal angiomyolipoma volume during rapamycin therapy (3, 14). However, approximately 1 year after treatment withdrawal, tumors reappeared and reached approximately 86% of their original volume (3). Similarly, the rapamycin analog RAD001 attenuated renal tumor development in *TSC2*^{+/-} mice, and its withdrawal led to marked tumor regrowth (72). Our data demonstrate that 50-day rapamycin treatment in doses that were 4 to 10 times lower than those used in previously published reports (1 mg/kg versus 4 to 10 mg/kg) (59–61, 68, 72) had growth-inhibitory effects on TSC2-null tumors in nude mice and suppressed mTORC1 signaling

without induction of apoptosis. Not surprisingly, rapamycin withdrawal resulted in tumor recurrence within 1 week after the last treatment, with tumor regrowth reaching 10% of the animal body weight by day 41. Thus, our findings further demonstrate that rapamycin as a single agent has limitations in inhibiting TSC2-null tumor growth and suggest that induction of apoptosis in TSC2-null tumors should have therapeutic benefits.

Lamb and colleagues showed that TSC1, which forms a tumor suppressor complex with TSC2, promotes stress fiber formation through activation of RhoA GTPase (56). We demonstrate that TSC2 loss induces TSC1-dependent stress fiber formation due to activation of RhoA GTPase that is rapamycin insensitive (27, 31). Rapamycin-insensitive mTORC2 regulates the actin cytoskeleton and Rho GTPase activity (44, 75), suggesting that mTORC2 may play a role in modulating Rho activity and Rho-dependent stress fiber formation due to TSC2 loss. Here, we demonstrate that the mTOR and rictor, but not raptor, are required for stress fiber formation in TSC2-null cells and that rictor regulates the activity of RhoA GTPase. Activated Rho rescued rictor-induced stress fiber disassembly in TSC2-null cells, demonstrating that rictor acts upstream of RhoA in regulating its activity and stress fiber formation due to TSC2 loss.

Rho GTPases have prosurvival and antiproliferative effects in different diseases, including human cancers (47, 74). We show that RhoA GTPase is necessary for TSC2-null cell proliferation and survival, and either RhoA knockdown or specific inhibition of Rho activity significantly inhibits proliferation and induces apoptosis in TSC2-null and LAM cells in an mTORC1-independent manner. Importantly, inhibition of mTORC2 signaling with siRNA for rictor markedly inhibited TSC2-null cell proliferation at levels comparable to those of siRNA for raptor, while it had little effect on mTORC1-dependent S6 phosphorylation. Importantly, constitutively active Rho rescued rictor siRNA-induced inhibition of proliferation, suggesting that mTORC2 modulates TSC2-null cell proliferation via Rho GTPase. Thus, our data show that TSC2 loss, in addition to activation of mTORC1, leads to mTORC2-dependent activation of RhoA GTPase, which acts as a prosurvival molecule and is required for the proliferation of TSC2-null cells. Thus, these data suggest that therapeutic targeting of RhoA may inhibit abnormal cell growth due to TSC2 loss and promote apoptosis in TSC2-null cells.

Extensive efforts have been made to develop selective Rho inhibitors; however, to date, none have been approved for

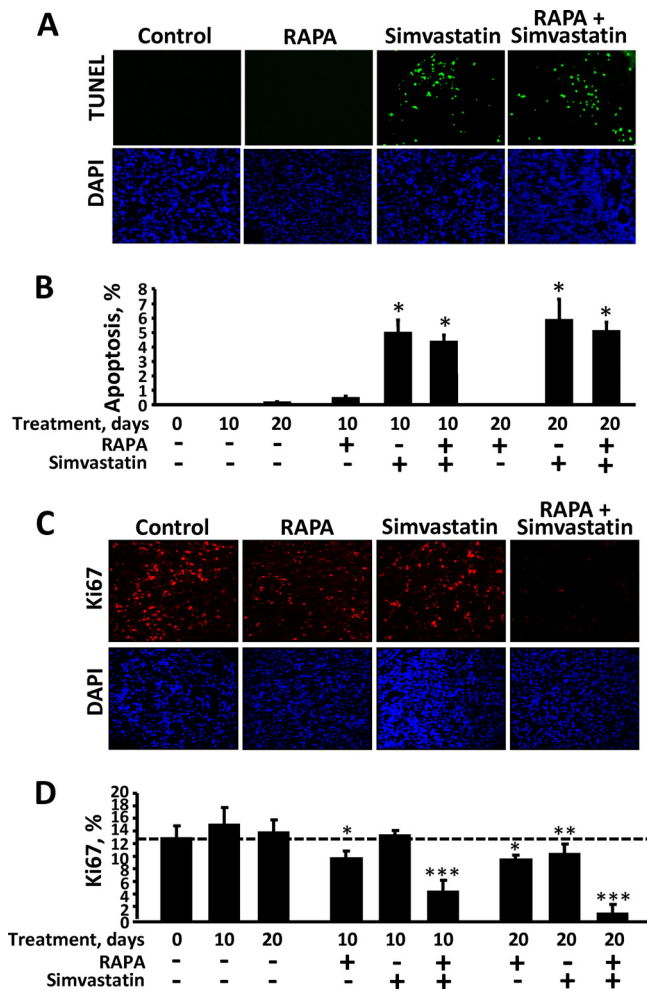


FIG. 10. (A and B) Simvastatin promotes apoptosis in TSC2-null tumors. Tumor tissues collected at days 0, 10, and 20 of the experiment were analyzed using the *In Situ* Cell Death Detection Kit (green); DAPI staining (blue) was performed to detect nuclei. (A) Representative images of tumors collected at day 20 of treatment were taken using an Eclipse TE2000-E microscope at $\times 200$ magnification with appropriate filters. (B) Statistical analysis. The data (mean values \pm SE; tumors from a minimum of five animals per treatment condition were analyzed) represent the percentage of apoptotic cells per total number of cells (taken as 100%). A minimum of 300 cells were analyzed per condition in each tumor. *, $P < 0.001$ for simvastatin on day 10 versus the control on day 10, for simvastatin on day 10 versus RAPA on day 10, for RAPA plus simvastatin on day 10 versus the control on day 10, for RAPA plus simvastatin on day 10 versus RAPA on day 10, for simvastatin on day 20 versus the control on day 20, for simvastatin on day 20 versus RAPA on day 20, for RAPA plus simvastatin on day 20 versus the control on day 20, and for RAPA plus simvastatin on day 20 versus RAPA on day 20 by ANOVA (Bonferroni-Dunn). (C and D) Simvastatin and rapamycin inhibit TSC2-null cell growth *in vivo*. Tumor tissues were collected on days 0, 10, and 20 of the experiment and subjected to immunohistochemical analysis with anti-Ki67 antibody (red). DAPI staining (blue) was performed to detect nuclei. (C) Representative images of tumors collected at day 20 of treatment were taken using an Eclipse E400 microscope at $\times 200$ magnification with appropriate filters. (D) Statistical analysis. The data (mean values \pm SE; tumors from a minimum of five animals per treatment condition were analyzed) represent the percentage of Ki67-positive cells per total number of cells (taken as 100%). A minimum of 300 cells were analyzed per condition in each tumor. *, $P < 0.01$ for RAPA on day 10 versus the control on day 10 and for RAPA on day 20 versus the control on day 20; **, $P < 0.05$ for simvastatin on day 20 versus the

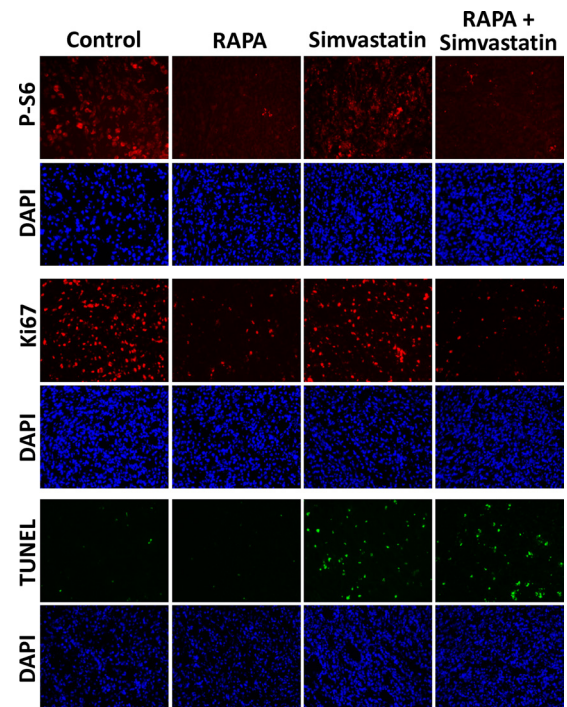


FIG. 11. TSC2-null tumors collected from control and rapamycin (RAPA)-, simvastatin-, and RAPA plus simvastatin-treated mice at days 45, 41, 34, and 32 of the experiment, respectively, were subjected to immunohistochemical analysis with anti-P-S6 (red) and anti-Ki67 (red) antibodies; apoptosis was examined using a TUNEL-based *In Situ* Death Detection Kit (green). DAPI staining (blue) was performed to detect nuclei. The images were taken using an Eclipse E400 microscope at $\times 200$ magnification with appropriate filters.

clinical use (74). Rho GTPases require prenylation (geranylgeranylation) for membrane binding and activation. Statins, which are HMG-CoA reductase inhibitors, suppress GGPP production, leading to nonselective inhibition of Rho GTPases. Statins, which are widely used clinically to reduce cholesterol levels (89), also have an oncoprotective effect in humans (15, 49, 70, 91) and inhibit proliferation and promote apoptosis in different cancer cells (4, 10, 23); a natural statin, simvastatin, induces apoptosis in numerous human cancer cell lines via suppression of RhoA GTPase activity (10, 23, 92).

We show that simvastatin inhibited Rho GTPase activity, attenuated proliferation, induced cleavage of caspase 3, and promoted apoptosis in TSC2-null cells. Importantly, the constitutively active Rho prevented simvastatin-induced caspase 3 cleavage, suggesting that simvastatin inhibits TSC2-related cell proliferation and promotes apoptosis via inhibition of Rho GTPase. In TSC2-null and LAMD cells, the RhoA-dependent apoptotic response involves downregulation of antiapoptotic Bcl2 and upregulation of proapoptotic Bim, Bok, and Puma.

control on day 20; ***, $P < 0.01$ for RAPA plus simvastatin on day 10 versus RAPA on day 10, for RAPA plus simvastatin on day 10 versus simvastatin on day 10, for RAPA plus simvastatin on day 20 versus RAPA on day 20, and for RAPA plus simvastatin on day 20 versus simvastatin on day 20 by ANOVA (Bonferroni-Dunn).

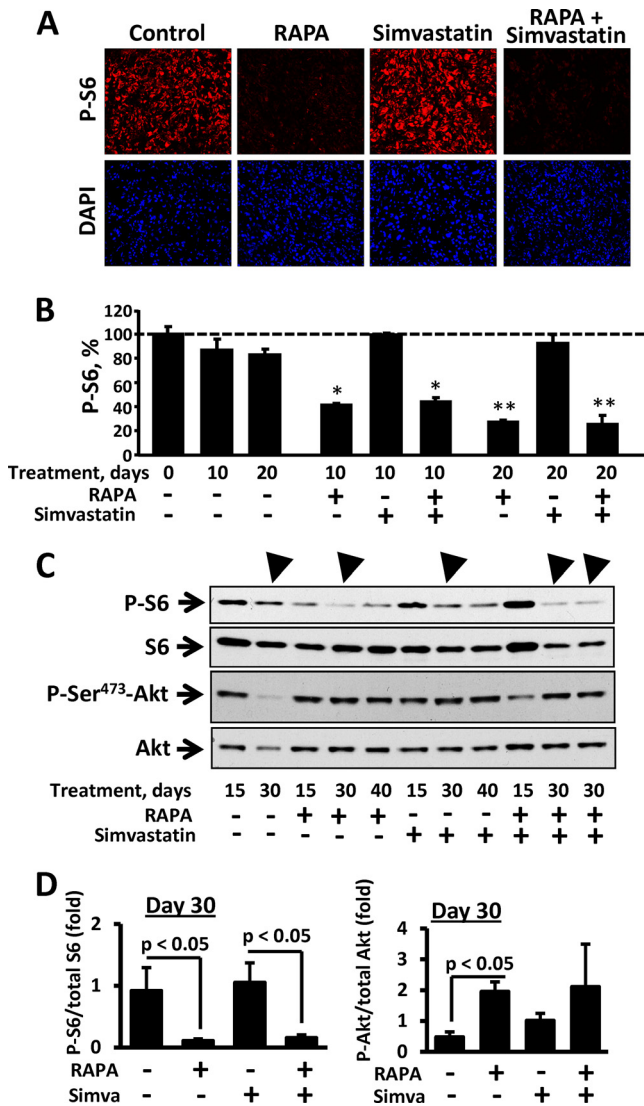


FIG. 12. Rapamycin, but not simvastatin, inhibits S6 phosphorylation in TSC2-null tumors. (A and B) Tumor tissues collected at days 0, 10, and 20 of the experiment were subjected to immunocytochemical analysis with anti-phospho-S6 antibody (red). DAPI staining (blue) was performed to detect nuclei. (A) Representative images of tumors collected at day 20 of treatment were taken using an Eclipse TE2000-E microscope at $\times 200$ magnification with appropriate filters. (B) Statistical analysis. The data represent mean values \pm SE; tumors from a minimum of five animals per treatment condition were analyzed. The P-S6 OD at day 0 was taken as 100%. *, $P < 0.001$ for rapamycin (RAPA) on day 10 versus the control on day 10; **, $P < 0.001$ for RAPA on day 20 versus the control on day 20 and for RAPA plus simvastatin on day 20 versus the control on day 20 by ANOVA (Bonferroni-Dunn). (C) Immunoblot analysis of tumor tissues collected at days 15, 30, and 40 of the experiment with anti-phospho-S6, anti-S6, anti-phospho-Akt(Ser-473), and anti-Akt antibodies. Representative images from three independent experiments are shown. The arrowheads indicate tissues collected at day 30 of the experiment. (D) Statistical analysis of tissues collected at day 30 of the experiment. The data are mean values \pm SE from three independent experiments by ANOVA (Bonferroni-Dunn).

Further, simvastatin attenuated TSC2-null subcutaneous tumor growth in nude mice and prolonged animal survival. Interestingly, simvastatin-dependent inhibition of tumor growth, which was observed after 12 days of simvastatin treatment, correlates with statin pharmacokinetic studies (62). Importantly, simvastatin promoted apoptosis and attenuated proliferation while it had little effect on mTORC1 signaling, confirming that the effects of simvastatin are mTORC1 independent. Although a relatively high dose of simvastatin was used in this study, because mice metabolize simvastatin more rapidly than humans, lower doses may be effective in humans (48).

Consistent with our *in vivo* findings, simvastatin inhibited proliferation, induced apoptosis, and cooperated with rapamycin in the inhibition of TSC2-null ELT3 cell growth *in vitro*. Importantly, similar data were obtained for primary LAMD cells dissociated from the nodules from the lungs of LAM patients (30, 32), suggesting that our findings may be applicable to LAM disease. The concentrations of simvastatin that inhibited growth and induced apoptosis in TSC2-null ELT3 and LAMD cells (0.3 to 1 μ M) were comparable to the plasma levels of statins achieved in humans in clinical trials ($2.32 \pm 1.27 \mu$ M at peak concentration) (86) and did not result in severe drug toxicity in the patients (91). Because rapamycin elevates triglycerides and total cholesterol levels (69), statins are routinely used in rapamycin-treated transplant patients to decrease the risk of cardiovascular disease and prolong survival (2, 78), and studies show no significant pharmacokinetic drug-drug interactions between rapamycin and statins (53, 96).

We demonstrate that simvastatin and rapamycin cooperated in inhibiting TSC2-null and LAMD cell proliferation *in vitro*, in reducing TSC2-null tumor size, and in improving tumor-bearing mouse survival *in vivo*. The combination of simvastatin and rapamycin induced apoptosis, inhibited mTORC1 signaling, and abrogated DNA synthesis in TSC2-null tumors. Importantly, in contrast to rapamycin-treated mice, which demonstrated marked tumor recurrence after rapamycin withdrawal, no tumor regrowth was detected in simvastatin- and simvastatin-rapamycin-treated mice during 9 months of observation following the last treatment. Taken together, these data demonstrate that the combination of cytostatic rapamycin with proapoptotic simvastatin improves survival, suppresses tumor growth, and prevents tumor regrowth upon treatment withdrawal.

Collectively, our data demonstrate that mTORC2-dependent RhoA GTPase activation is necessary for TSC2-null cell growth and survival. *In vivo* targeting of RhoA GTPase with simvastatin and mTORC1 with rapamycin abrogates TSC2-null tumor growth, induces apoptosis, increases tumor-bearing mouse survival, and prevents posttreatment tumor regrowth. Our findings have important implications, because they show RhoA GTPase is a potential therapeutic target for combinational therapy in diseases associated with TSC2 dysfunction.

ACKNOWLEDGMENTS

We thank our colleagues Yvonne Paterson, Reynold A. Panettieri, Jr., and Andrew Eszterhas for critical reading of the manuscript and helpful discussions; Margaret M. Chou for generously providing us with GST-V14Rho or control GST plasmids; Cheryl L. Walker, M. D. Anderson Cancer Center, University of Texas, Smithville, TX, for ELT3 cells; David Kwiatkowski, Brigham and Women's Hospital, Har-

vard University, Boston, MA, for *Tsc2^{-/-}*, *Tsc2^{+/+}*, *Tsc2^{+/+} p53^{-/-}*, and *Tsc2^{-/-} p53^{-/-}* MEFs; and the National Disease Research Interchange (NDRI) for providing us with LAM tissue.

This work is supported by grants from the NIH/NHLBI (2RO1HL071106 [V.P.K.], RO1HL090829 [V.P.K.], and ALA CI-9813-N [V.P.K.]) and the LAM Foundation (V.P.K.), by Abramson Cancer Center Core Support Grant NIH P130-CA-016520-34 (V.P.K.), and by ATS/LAM Foundation research grant LAM-07-001 (E.A.G.) and in part by a Gilead Science Research Scholars grant (E.A.G.). E.A.G. is a Parker B. Francis Fellow in Pulmonary Research.

REFERENCES

- Ahn, K. S., G. Sethi, and B. B. Aggarwal. 2008. Reversal of chemoresistance and enhancement of apoptosis by statins through down-regulation of the NF- κ B pathway. *Biochem. Pharmacol.* **75**:907–913.
- Aliabadi, A. Z., et al. 2008. Safety and efficacy of statin therapy in patients switched from cyclosporine to sirolimus after cardiac transplantation. *Transplantation* **86**:1771–1776.
- Bissler, J. J., et al. 2008. Sirolimus for angiomyolipoma in tuberous sclerosis complex or lymphangioleiomyomatosis. *N. Engl. J. Med.* **358**:140–151.
- Blanco-Colio, L. M., et al. 2002. 3-Hydroxy-3-methyl-glutaryl coenzyme A reductase inhibitors, atorvastatin and simvastatin, induce apoptosis of vascular smooth muscle cells by downregulation of Bcl-2 expression and Rho A prenylation. *Atherosclerosis* **161**:17–26.
- Breuleux, M., et al. 2009. Increased AKT S473 phosphorylation after mTORC1 inhibition is rictor dependent and does not predict tumor cell response to PI3K/mTOR inhibition. *Mol. Cancer Ther.* **8**:742–753.
- Budman, D. R., J. Tai, and A. Calabro. 2007. Fluvastatin enhancement of trastuzumab and classical cytotoxic agents in defined breast cancer cell lines in vitro. *Breast Cancer Res. Treat.* **104**:93–101.
- Cafforio, P., F. Dammacco, A. Gernone, and F. Silvestris. 2005. Statins activate the mitochondrial pathway of apoptosis in human lymphoblasts and myeloma cells. *Carcinogenesis* **26**:883–891.
- Calabro, A., J. Tai, S. L. Allen, and D. R. Budman. 2008. In-vitro synergism of m-TOR inhibitors, statins, and classical chemotherapy: potential implications in acute leukemia. *Anticancer Drugs* **19**:705–712.
- Castro, A. F., J. F. Rebhun, G. G. Clark, and L. A. Quilliam. 2003. Rheb binds TSC2 and promotes S6 kinase activation in a rapamycin- and farnesylation-dependent manner. *J. Biol. Chem.* **278**:32493–32496.
- Cho, S.-J., et al. 2008. Simvastatin induces apoptosis in human colon cancer cells and in tumor xenografts, and attenuates colitis-associated colon cancer in mice. *Int. J. Cancer* **123**:951–957.
- Coleman, K., C. J. Marshal, and M. F. Olson. 2004. Ras and Rho GTPases in G₁-phase cell-cycle regulation. *Nat. Rev. Mol. Cell Biol.* **5**:355–366.
- Copp, J., G. Manning, and T. Hunter. 2009. TORC-specific phosphorylation of mammalian target of rapamycin (mTOR): phospho-Ser2481 is a marker for intact mTOR signaling complex 2. *Cancer Res.* **69**:1821–1827.
- Costello, P. S., S. C. Cleverley, R. Galandrimi, S. W. Henning, and D. A. Cantrell. 2000. The GTPase rho controls a p53-dependent survival checkpoint during thymopoiesis. *J. Exp. Med.* **192**:77–85.
- Davies, D. M., et al. 2008. Sirolimus therapy in tuberous sclerosis or sporadic lymphangioleiomyomatosis. *N. Engl. J. Med.* **358**:200–203.
- Demierre, M.-F., P. D. R. Higgins, S. B. Gruber, E. Hawk, and S. M. Lippman. 2005. Statins and cancer prevention. *Nat. Rev. Cancer* **5**:930–942.
- Etienne-Manneville, S., and A. Hall. 2002. Rho GTPases in cell biology. *Nature* **420**:629–635.
- Ferri, N., et al. 2008. Fluvastatin synergistically improves the antiproliferative effect of everolimus on rat smooth muscle cells by altering p27Kip1/cyclin E expression. *Mol. Pharmacol.* **74**:144–153.
- Finlay, G. A., et al. 2007. Selective inhibition of growth of tuberous sclerosis complex 2 null cells by atorvastatin is associated with impaired Rheb and Rho GTPase function and reduced mTOR/S6 kinase activity. *Cancer Res.* **67**:9878–9886.
- Fiorentini, C., et al. 1998. Toxin-induced activation of Rho GTP-binding protein increases Bcl-2 expression and influences mitochondrial homeostasis. *Exp. Cell Res.* **242**:341–350.
- Foster, K. G., and D. C. Fingar. 2010. Mammalian Target of Rapamycin (mTOR): conducting the cellular signaling symphony. *J. Biol. Chem.* **285**:14071–14077.
- Franz, D. N., et al. 2006. Rapamycin causes regression of astrocytomas in tuberous sclerosis complex. *Ann. Neurol.* **59**:490–498.
- Fromigué, O., et al. 2006. RhoA GTPase inactivation by statins induces osteosarcoma cell apoptosis by inhibiting p42/p44-MAPKs-Bcl-2 signaling independently of BMP-2 and cell differentiation. *Cell Death Differ.* **13**:1845–1856.
- Fuchs, D., C. Berges, G. Opelz, V. Daniel, and C. Naujokat. 2008. HMG-CoA reductase inhibitor simvastatin overcomes bortezomib-induced apoptosis resistance by disrupting a geranylgeranyl pyrophosphate-dependent survival pathway. *Biochem. Biophys. Res. Commun.* **374**:309–314.
- Garami, A., et al. 2003. Insulin activation of Rheb, a mediator of mTOR/S6K/4E-BP signaling, is inhibited by TSC1 and 2. *Mol. Cell* **11**:1457–1466.
- Ghosh-Choudhury, N., C. C. Mandal, N. Ghosh-Choudhury, and G. Ghosh Choudhury. 2010. Simvastatin induces derepression of PTEN expression via NF κ B to inhibit breast cancer cell growth. *Cell. Signal.* **22**:749–758.
- Gómez, J., C. Martínez-A. M. Giry, A. García, and A. Rebollo. 1997. Rho prevents apoptosis through Bcl-2 expression: implications for interleukin-2 receptor signal transduction. *Eur. J. Immunol.* **27**:2793–2799.
- Goncharova, E., D. Goncharov, D. Noonan, and V. P. Krymskaya. 2004. TSC2 modulates actin cytoskeleton and focal adhesion through TSC1-binding domain and the Rac1 GTPase. *J. Cell Biol.* **167**:1171–1182.
- Goncharova, E. A., et al. 2008. Interferon β augments tuberous sclerosis complex 2 (TSC2)-dependent inhibition of TSC2-null ELT3 and human lymphangioleiomyomatosis-derived cell proliferation. *Mol. Pharmacol.* **73**:778–788.
- Goncharova, E. A., et al. 2009. STAT3 is required for abnormal proliferation and survival of TSC2-deficient cells: relevance to pulmonary LAM. *Mol. Pharmacol.* **76**:766–777.
- Goncharova, E. A., et al. 2002. Tuberin regulates p70 S6 kinase activation and ribosomal protein S6 phosphorylation: a role for the TSC2 tumor suppressor gene in pulmonary lymphangioleiomyomatosis (LAM). *J. Biol. Chem.* **277**:30958–30967.
- Goncharova, E. A., D. A. Goncharov, P. N. Lim, D. Noonan, and V. P. Krymskaya. 2006. Modulation of cell migration and invasiveness by tumor suppressor TSC2 in lymphangioleiomyomatosis. *Am. J. Respir. Cell Mol. Biol.* **34**:473–480.
- Goncharova, E. A., et al. 2006. Abnormal smooth muscle cell growth in lymphangioleiomyomatosis (LAM): role for tumor suppressor TSC2. *Am. J. Respir. Cell Mol. Biol.* **34**:561–572.
- Goncharova, E. A., and V. P. Krymskaya. 2008. Pulmonary lymphangioleiomyomatosis (LAM): progress and current challenges. *J. Cell. Biochem.* **103**:369–382.
- Goncharova, E. A., P. Lin, D. A. Goncharov, A. Eszterhas, R. A. Panettieri, Jr., and V. P. Krymskaya. 2006. Assays for in vitro monitoring proliferation of human airway smooth muscle (ASM) and human pulmonary arterial vascular smooth muscle (VSM) cells. *Nat. Protoc.* **1**:2905–2908.
- Guertin, D. A., and D. M. Sabatini. 2009. The pharmacology of mTOR inhibition. *Sci. Signal.* **2**:pe24.
- Guertin, D. A., et al. 2006. Ablation in mice of the mTORC components raptor, rictor, or mLST8 reveals that mTORC2 is required for signaling to Akt-FOXO and PKC[α], but not S6K1. *Dev. Cell* **11**:859–871.
- Harrington, L. S., et al. 2004. The TSC1-2 tumor suppressor controls insulin-PI3K signaling via regulation of IRS proteins. *J. Cell Biol.* **166**:213–223.
- Howe, S. R., et al. 1995. Rodent model of reproductive tract leiomyomata. Establishment and characterization of tumor-derived cell lines. *Am. J. Pathol.* **146**:1568–1579.
- Hsu, S. Y., A. I. Kaipia, E. McGee, M. Lomeli, and A. J. W. Hsueh. 1997. Bok is a pro-apoptotic Bcl-2 protein with restricted expression in reproductive tissues and heterodimerizes with selective anti-apoptotic Bcl-2 family members. *Proc. Natl. Acad. Sci. U. S. A.* **94**:12401–12406.
- Huang, J., C. C. Dibble, M. Matsuzaki, and B. D. Manning. 2008. The TSC1-TSC2 complex is required for proper activation of mTOR complex 2. *Mol. Cell Biol.* **28**:4104–4115.
- Huynh, H., C. Teo, and K. Soo. 2007. Bevacizumab and rapamycin inhibit tumor growth in peritoneal model of human ovarian cancer. *Mol. Cancer Ther.* **6**:2959–2966.
- Hwang, K. E., et al. 13 May 2010. Apoptotic induction by simvastatin in human lung cancer A549 cells via Akt signaling dependent down-regulation of survivin. *Invest. New Drugs.* [Epub ahead of print.] doi:10.1007/s10637-010-9450-2.
- Inoki, K., Y. Li, T. Xu, and K.-L. Guan. 2003. Rheb GTPase is a direct target of TSC2 GAP activity and regulates mTOR signaling. *Genes Dev.* **17**:1829–1834.
- Jacinto, E., et al. 2004. Mammalian TOR complex 2 controls the actin cytoskeleton and is rapamycin insensitive. *Nat. Cell Biol.* **6**:1122–1128.
- Jaffe, A. B., and A. Hall. 2005. RHO GTPASES: biochemistry and biology. *Annu. Rev. Cell Dev. Biol.* **21**:247–269.
- Johnson, S. R. 2006. Lymphangioleiomyomatosis. *Eur. Respir. J.* **27**:1056–1065.
- Karlsson, R., E. D. Pedersen, Z. Wang, and C. Brakebusch. 2009. Rho GTPase function in tumorigenesis. *Biochim. Biophys. Acta* **1796**:91–98.
- Katano, H., L. Pesnicak, and J. I. Cohen. 2004. Simvastatin induces apoptosis of Epstein-Barr virus (EBV)-transformed lymphoblastoid cell lines and delays development of EBV lymphomas. *Proc. Natl. Acad. Sci. U. S. A.* **101**:4960–4965.
- Kawata, S., et al. 2001. Effect of pravastatin on survival in patients with advanced hepatocellular carcinoma. A randomized controlled trial. *Br. J. Cancer* **84**:886–891.
- Kenerson, H., T. A. Dundon, and R. S. Yeung. 2005. Effects of rapamycin in the Eker rat model of tuberous sclerosis complex. *Pediatr. Res.* **57**:67–75.
- Knudson, A. G. 2000. Chasing the cancer demon. *Annu. Rev. Genet.* **34**:1–19.
- Kochuparambil, S. T., B. Al-Husein, A. Goc, S. Soliman, and P. R. Somanath. 2011. Anticancer efficacy of simvastatin on prostate cancer cells and tumor xenografts is associated with inhibition of Akt and re-

- duced prostate-specific antigen expression. *J. Pharmacol. Exp. Ther.* **336**:496–505.
53. Kovarik, J. M., C. Hsu, L. McMahon, S. Berthier, and C. Rordorf. 2001. Population pharmacokinetics of everolimus in de novo renal transplant patients: impact of ethnicity and comedications. *Clin. Pharmacol. Ther.* **70**:247–254.
 54. Krymskaya, V. P., and E. A. Goncharova. 2009. PI3K/mTORC1 activation in hamartoma syndromes: therapeutic prospects. *Cell Cycle* **8**:403–413.
 55. Krymskaya, V. P., et al. 2 March 2011. mTOR is required for pulmonary arterial vascular smooth muscle cell proliferation under chronic hypoxia. *FASEB J.* [Epub ahead of print.] doi: 10.1096/fj.10-175018.
 56. Lamb, R. F., et al. 2000. The TSC1 tumour suppressor hamartin regulates cell adhesion through ERM proteins and the GTPase Rho. *Nat. Cell Biol.* **2**:281–287.
 57. Laplante, M., and D. M. Sabatini. 2009. mTOR signaling at a glance. *J. Cell Sci.* **122**:3589–3594.
 58. Laufs, U., D. Marra, K. Node, and J. K. Liao. 1999. 3-Hydroxy-3-methylglutaryl-CoA reductase inhibitors attenuate vascular smooth muscle proliferation by preventing Rho GTPase-induced down-regulation of p27Kip1. *J. Biol. Chem.* **274**:21926–21931.
 59. Lee, L., P. Sudentas, and S. L. Dabora. 2006. Combination of a rapamycin analog (CCI-779) and interferon-gamma is more effective than single agents in treating a mouse model of tuberous sclerosis complex. *Genes Chromosomes Cancer* **45**:933–944.
 60. Lee, L., et al. 2005. Efficacy of a rapamycin analog (CCI-779) and IFN-gamma in tuberous sclerosis mouse models. *Genes Chromosomes Cancer* **42**:213–227.
 61. Lee, N., et al. 2009. Rapamycin weekly maintenance dosing and the potential efficacy of combination sorafenib plus rapamycin but not atorvastatin or doxycycline in tuberous sclerosis preclinical models. *BMC Pharmacol.* **9**:8.
 62. Lennernäs, H., and G. Fager. 1997. Pharmacodynamics and pharmacokinetics of the HMG-CoA reductase inhibitors. Similarities and differences. *Clin. Pharmacokinet.* **32**:403–425.
 63. Li, Y., M. N. Corradetti, K. Inoki, and K.-L. Guan. 2004. TSC2: filling the GAP in the mTOR signaling pathway. *Trends Biochem. Sci.* **29**:32–38.
 64. Loewith, R., et al. 2002. Two TOR complexes, only one of which is rapamycin sensitive, have distinct roles in cell growth control. *Mol. Cell* **10**:457–468.
 65. Long, X., S. Ortiz-Vega, Y. Lin, and J. Avruch. 2005. Rheb binding to mammalian target of rapamycin (mTOR) is regulated by amino acid sufficiency. *J. Biol. Chem.* **280**:23433–23436.
 66. Maeda, A., et al. 2010. Down-regulation of RhoA is involved in the cytotoxic action of lipophilic statins in HepG2 cells. *Atherosclerosis* **208**:112–118.
 67. Mahalati, K., and B. D. Kahan. 2001. Clinical pharmacokinetics of sirolimus. *Clin. Pharmacokinet.* **40**:573–585.
 68. Messina, M. P., A. Rauktys, L. Lee, and S. L. Dabora. 2007. Tuberous sclerosis preclinical studies: timing of treatment, combination of a rapamycin analog (CCI-779) and interferon-gamma, and comparison of rapamycin to CCI-779. *BMC Pharmacol.* **7**:14.
 69. Murgia, M. G., S. Jordan, and B. D. Kahan. 1996. The side effect profile of sirolimus: a phase I study in quiescent cyclosporine-prednisone-treated renal transplant patients. *Kidney Int.* **49**:209–216.
 70. Murtola, T. J., T. Visakorpi, J. Lahtela, H. Syvala, and T. L. J. Tammela. 2008. Statins and prostate cancer prevention: where we are now, and future directions. *Nat. Clin. Pract. Urol.* **5**:376–387.
 71. Nonaka, M., et al. 2009. Role for protein geranylgeranylation in adult T-cell leukemia cell survival. *Exp. Cell Res.* **315**:141–150.
 72. Pollizzi, K., I. Malinowska-Kolodziej, M. Stumm, H. Lane, and D. Kwiatkowski. 2009. Equivalent benefit of mTORC1 blockade and combined PI3K-mTOR blockade in a mouse model of tuberous sclerosis. *Mol. Cancer* **8**:38.
 73. Rattan, R., S. Giri, A. K. Singh, and I. Singh. 2006. Rho/ROCK pathway as a target of tumor therapy. *J. Neurosci. Res.* **83**:243–255.
 74. Sahai, E., and C. J. Marshall. 2002. Rho-GTPases and cancer. *Nat. Rev. Cancer* **2**:133–142.
 75. Sarbassov, D. D., et al. 2004. Rictor, a novel binding partner of mTOR, defines a rapamycin-insensitive and raptor-independent pathway that regulates the cytoskeleton. *Curr. Biol.* **14**:1296–1302.
 76. Schmelzel, T., and M. N. Hall. 2000. TOR, a central controller of cell growth. *Cell* **103**:253–262.
 77. Schmidt, A., M. Bickle, T. Beck, and M. N. Hall. 1997. The yeast phosphatidylinositol kinase homolog TOR2 activates RHO1 and RHO2 via the exchange factor ROM2. *Cell* **88**:531–542.
 78. Schonder, K. S., T. P. McKaveney, and K. J. Lynch. 2005. Retrospective analysis of hyperlipidemia management in a transplant population. *Pharmacotherapy* **25**:918–923.
 79. Schoonjans, K., et al. 1999. 3-Hydroxy-3-methylglutaryl CoA reductase inhibitors reduce serum triglyceride levels through modulation of apolipoprotein C-III and lipoprotein lipase. *FEBS Lett.* **452**:160–164.
 80. Shah, O. J., Z. Wang, and T. Hunter. 2004. Inappropriate activation of the TSC/Rheb/mTOR/S6K cassette induces IRS1/2 depletion, insulin resistance, and cell survival deficiencies. *Curr. Biol.* **14**:1650–1656.
 81. Shiota, C., J. Woo, J. Lindner, K. D. Shelton, and M. A. Magnuson. 2006. Multiallelic disruption of the rictor gene in mice reveals that mTOR complex 2 is essential for fetal growth and viability. *Dev. Cell* **11**:583–589.
 82. Soliman, G. A., et al. 2010. mTOR Ser-2481 autophosphorylation monitors mTORC-specific catalytic activity and clarifies rapamycin mechanism of action. *J. Biol. Chem.* **285**:7866–7879.
 83. Sun, S. Y., et al. 2005. Activation of Akt and eIF4E survival pathways by rapamycin-mediated mammalian target of rapamycin inhibition. *Cancer Res.* **65**:7052–7058.
 84. Takeda, N., et al. 2006. Role of RhoA inactivation in reduced cell proliferation of human airway smooth muscle by simvastatin. *Am. J. Respir. Cell Mol. Biol.* **35**:722–729.
 85. Taveira-DaSilva, A. M., and J. Moss. 2006. Lymphangioleiomyomatosis. *Cancer Control* **13**:276–285.
 86. Thibault, A., et al. 1996. Phase I study of lovastatin, an inhibitor of the mevalonate pathway, in patients with cancer. *Clin. Cancer Res.* **2**:483–491.
 87. Torrance, C. J., V. Agrawal, B. Vogelstein, and K. W. Kinzler. 2001. Use of isogenic human cancer cells for high-throughput screening and drug discovery. *Nat. Biotechnol.* **19**:940–945.
 88. Um, S. H., et al. 2004. Absence of S6K1 protects against age- and diet-induced obesity while enhancing insulin sensitivity. *Nature* **431**:200–205.
 89. Vaughan, C. J., and A. M. Gotto, Jr. 2004. Update on statins: 2003. *Circulation* **110**:886–892.
 90. von Tresckow, B., et al. 2007. Simvastatin-dependent apoptosis in Hodgkin's lymphoma cells and growth impairment of human Hodgkin's tumors in vivo. *Haematologica* **92**:682–685.
 91. Wong, W. W., J. Dimitroulakos, M. D. Minden, and L. Z. Penn. 2002. HMG-CoA reductase inhibitors and the malignant cell: the statin family of drugs as triggers of tumor-specific apoptosis. *Leukemia* **16**:508–519.
 92. Wu, J., W. W. Wong, F. Khosravi, M. D. Minden, and L. Z. Penn. 2004. Blocking the Raf/MEK/ERK pathway sensitizes acute myelogenous leukemia cells to lovastatin-induced apoptosis. *Cancer Res.* **64**:6461–6468.
 93. Yeung, R. S. 2003. Multiple roles of the tuberous sclerosis complex genes. *Genes Chromosomes Cancer* **38**:368–375.
 94. Zhang, H., et al. 2003. Loss of Tsc1/Tsc2 activates mTOR and disrupts PI3K-Akt signaling through downregulation of PDGFR. *J. Clin. Invest.* **112**:1223–1233.
 95. Zhang, Y., et al. 2003. Rheb is a direct target of the tuberous sclerosis tumour suppressor proteins. *Nat. Cell Biol.* **5**:578–581.
 96. Zimmerman, J. J. 2004. Exposure-response relationships and drug interactions of sirolimus. *AAPS J.* **6**:e28.